

**ECONOMIC GEOLOGY  
RESEARCH UNIT**

University of the Witwatersrand  
Johannesburg

---

A GEOCHEMICAL STUDY OF  
PSEUDOTACHYLITIC BRECCIAS  
FROM FAULT ZONES IN THE  
WITWATERSRAND BASIN, SOUTH AFRICA

**W.U. REIMOLD, C. KOEBERL, P. FLETCHER,  
A.M. KILLICK AND J.D. WILSON**

---

• INFORMATION CIRCULAR No. 324

UNIVERSITY OF THE WITWATERSRAND  
JOHANNESBURG

**A GEOCHEMICAL STUDY OF PSEUDOTACHYLITIC BRECCIAS FROM FAULT  
ZONES IN THE WITWATERSRAND BASIN, SOUTH AFRICA**

by

**W.U. REIMOLD<sup>1</sup>, C. KOEBERL<sup>2</sup>, P. FLETCHER<sup>3</sup>, A.M. KILLICK<sup>4</sup>, and J.D.  
WILSON<sup>5</sup>**

(<sup>1</sup>Department of Geology, University of the Witwatersrand, Private Bag 3, P.O. Wits 2050, Johannesburg, South Africa, <sup>2</sup>Institute for Geochemistry, University of Vienna, Althanstrasse 14, A-1090 Vienna, Austria, <sup>3</sup>14 Vrede Street, Fochville 2515, South Africa, <sup>4</sup>JCI Limited, P.O. Box 590, Johannesburg 2000, South Africa, <sup>5</sup>CORSTOR Pty. Limited, P.O. Box 1551, Fourways 2055, South Africa)

**ECONOMIC GEOLOGY RESEARCH UNIT  
INFORMATION CIRCULAR No. 324**

**June, 1998**

## **A GEOCHEMICAL STUDY OF PSEUDOTACHYLITIC BRECCIAS FROM FAULT ZONES IN THE WITWATERSRAND BASIN, SOUTH AFRICA**

### **ABSTRACT**

Pseudotachylitic breccias, associated with either bedding-parallel or normal faults, are abundant in the northern and northwestern parts of the gold- and uranium-rich Witwatersrand Basin in South Africa. They occur particularly abundantly in a zone tangential to the Vredefort Dome, which has now been widely accepted as the eroded remnant of the central uplift of the originally 300km-wide Vredefort impact structure.

Several of these fault zones were sampled along traverses that include both fault breccias and host rocks. Geochemical analyses were undertaken to investigate the processes involved in fault rock formation. The temporal relationships of fault activity to regional geological events were also examined. Detailed petrographic analysis showed that the faults were strongly hydrothermally overprinted during autometasomatism related to breccia formation, as well as to post-formational alteration. Mixing between two or more precursor lithologies and fluid alteration can be shown to have affected both the fault zones and their wall-rocks. A wide spectrum of trace elements, including Au and U, was mobilised and redeposited by these processes.

The fault zones, some of which are of basin-wide significance, were important channels for fluids that modified the base metal content of the Witwatersrand Basin. That these processes affected at least a major part of the Basin can be gauged from the regionally separated locations of the study areas. However, as the chemical characteristics determined for the fault zones differ from site to site, it is likely that the metals were only locally remobilised and restricted to reef horizons in the vicinity of fault zones or to previously hydrothermally altered country rock. Subsequent redeposition of metals was limited to the regimes in and around such fault zones.

\_\_\_\_\_oOo\_\_\_\_\_

# A GEOCHEMICAL STUDY OF PSEUDOTACHYLITIC BRECCIAS FROM FAULT ZONES IN THE WITWATERSRAND BASIN, SOUTH AFRICA

## CONTENTS

	Page
<b>INTRODUCTION</b>	<b>1</b>
<b>SAMPLING AND SAMPLE PETROGRAPHY</b>	<b>3</b>
Petrographic observations	5
Experimental procedures	12
Results	12
1. <i>East Driefontein Section</i>	12
2. <i>Doornfontein Drillcore</i>	12
3. <i>Western Areas Suite</i>	15
(a) Major element analysis	15
(b) Trace element analysis	20
4. <i>Boskop Dam Drillcore</i>	21
<b>DISCUSSION AND CONCLUSIONS</b>	<b>25</b>
<b>ACKNOWLEDGEMENTS</b>	<b>28</b>
<b>REFERENCES</b>	<b>28</b>

—oOo—

Published by the Economic Geology Research Unit  
Department of Geology  
University of the Witwatersrand  
1 Jan Smuts Avenue  
Johannesburg 2001  
South Africa

ISBN 1-86838-214-1

# A GEOCHEMICAL STUDY OF PSEUDOTACHYLITIC BRECCIAS FROM FAULT ZONES IN THE WITWATERSRAND BASIN, SOUTH AFRICA

## INTRODUCTION

The Vredefort Dome, located approximately in the center of the Witwatersrand Basin (Fig. 1), is generally accepted as the erosional remnant of the central uplifted core of the world's largest and oldest known impact structure (e.g. Reimold and Gibson, 1996; Henkel and Reimold, 1998). The Dome is also known as the type locality for "pseudotachylite" (Shand, 1916). As Reimold (1995, 1998) discussed, this provides a major dilemma with regard to *what should be regarded as pseudotachylite*. Whereas tectonic workers generally reserve this term for fault breccia formed as friction melt (e.g. Magloughlin and Spray, 1992a; Reimold and Colliston, 1994; and references in these papers), various types of breccias in impact structure settings have been indiscriminately called pseudotachylite, regardless of whether or not they show evidence of any form of melting, either melting by fault activity, or impact melting. Reimold (1995, 1998) proposed that where a breccia shows a likeness to pseudotachylite, but where an origin as tectonic friction melt has not been proven, the term 'pseudotachylitic breccia' should be applied.

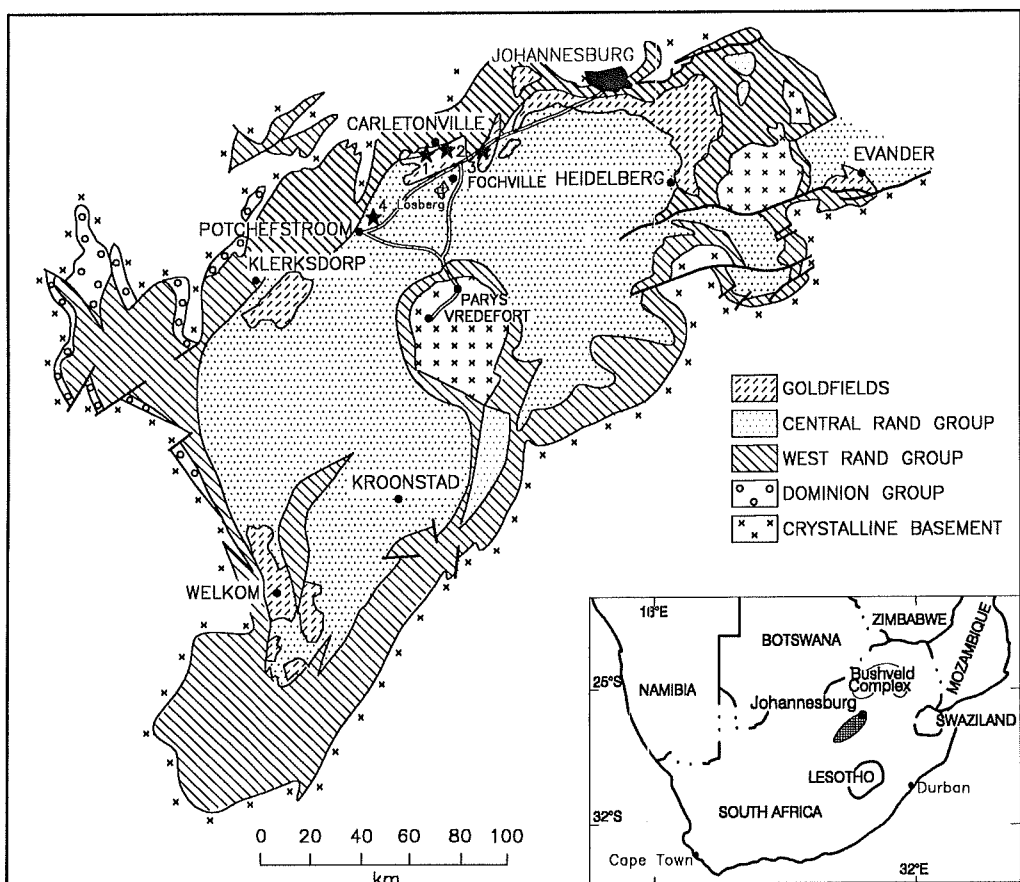
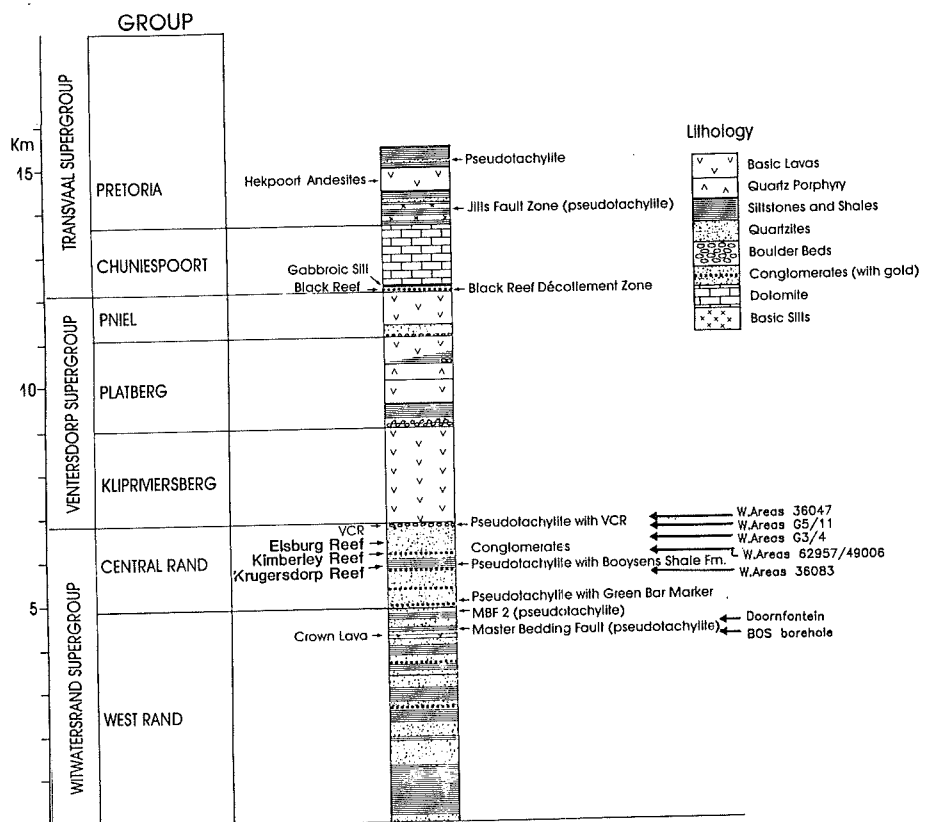


Figure 1: Locations of Doornfontein (1), East Driefontein (2) and Western Areas (3) gold mines and the drilling site of borehole BOS7 (4) in the northern Witwatersrand Basin.

Massive pseudotachylitic breccias are known only from two very large impact structures - Vredefort and the Sudbury Structure in Canada (e.g. Dressler, 1984; Grieve et al., 1991). In addition, abundant breccias have been described from the northern and northwestern parts of the Witwatersrand Basin (Fletcher and Reimold, 1989; Killick and Reimold, 1990; Reimold and Colliston, 1994; Killick and Roering, 1998), which according to Henkel and Reimold (1997, 1998), represent the impact ring basin of the Vredefort impact structure. Large, up to several tens of meters thick, breccia occurrences have been described from a number of bedding-parallel faults in Witwatersrand strata, between Witwatersrand and overlying Ventersdorp strata, and in Transvaal sediments (Fig. 2; these Supergroups collectively span the geological time period between about 2.9 and 2.3 Ga). In addition, pseudotachylitic breccias are known from several mainly north-south trending normal faults, such as the Bank Fault (BF), the West Rand Fault (WRF), and the Mooi River Fault (MRF) discussed by Fletcher and Reimold (1989). These authors also showed that known occurrences of massive pseudotachylitic breccias are concentrated along a tangent to the northern margin of the Vredefort Dome and are generally lacking from other parts of the Witwatersrand Basin.



*Figure 2: Schematic lithostratigraphic column for the Witwatersrand Basin (modified after Fletcher and Reimold, 1989), indicating prominent pseudotachylite-bearing fault zones and the stratigraphic horizons sampled in this study*

Killick and Reimold (1990) and Fletcher and Reimold (1989) concluded, on the basis of chemical and structural aspects of Vredefort and Witwatersrand pseudotachylitic breccias, that they might be related. Trieloff et al. (1994) presented initial radiometric age data for several breccia samples from the Ventersdorp Contact Reef (VCR) at the contact between the Witwatersrand and

Ventersdorp Supergroups. They proposed that the 2 Ga ages obtained for seven of their samples provided a tentative link to the Vredefort event. Since then, the Vredefort impact event has been dated by several groups at  $2020 \pm 5$  Ma (Spray et al., 1995; Kamo et al., 1996; Gibson et al., 1997), and it is widely believed that, at least, most of the Vredefort and Witwatersrand pseudotachylitic breccias were formed as a result of the Vredefort impact event (cf. also review by Reimold and Gibson, 1996). However, Berlenbach and Roering (1992) presented evidence for at least some pseudotachylitic breccia from the Witwatersrand Basin being as old as 2.7 Ga, and Reimold and Colliston (1994) also provided evidence suggesting some breccia pre-dated the impact event.

The early work on Witwatersrand and Vredefort pseudotachylitic breccias showed that significant hydrothermal effects were apparent within and adjacent to major fault zones. Reimold and Koeberl (1991) proposed that such fault zones could have acted as channels for basin-wide fluidisation. In order to investigate possible influences fluidisation may have had on the distribution of economically important base metals in the Basin - there can be no doubt that a significant proportion of Witwatersrand gold and associated sulphides have been remobilised since deposition (e.g. Robb and Meyer, 1991; Phillips and Myers, 1989; Boer et al., 1993a, b; Robb et al., 1997) - several fault breccia profiles were sampled for major and trace element analysis.

Any manifestation of major rock deformation and alteration in the Witwatersrand Basin, with a controversial origin for its gold resources still unresolved (e.g. Davidson, 1995; Minter et al., 1993; Robb and Meyer, 1995), is of major significance with regard to the geological evolution of this ore deposit.

## SAMPLING AND SAMPLE PETROGRAPHY

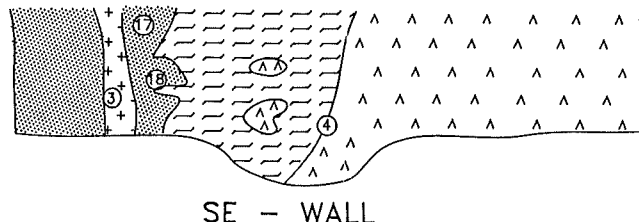
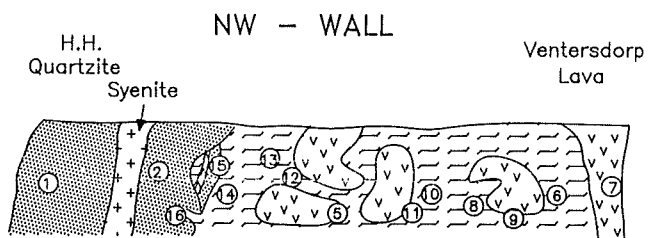
Detailed profiles were sampled at four localities in the northern Witwatersrand Basin (Fig. 1):

- (1) a part of borehole BB18 (Gold Fields of South Africa Ltd), which had been sunk into the northwestern portion of Doornfontein Gold Mine (southwest of the town of Carletonville). This drillcore intersects the upper part of the West Rand Group (Fig. 2) with the Master Bedding Fault (MBF, Fletcher and Reimold, 1989), which is well-known for its massive fault rock occurrences, including pseudotachylite, mylonitic and cataclastic breccias. The detailed stratigraphy of this 7m-thick drillcore section from approximately 1253 m depth is shown in Figure 3A. The breccia zone comprises several intersections of pseudotachylitic breccia, which are intercalated with quartzite, dolomite, mylonitic quartzite, and an altered mafic dyke cutting across the fault zone. The presence of dolomite of likely Transvaal age (2.5-2.25 Ga) places an upper age limit on the brecciation phase;
- (2) a crosscut on Level 20 in East Driefontein Gold Mine (EDGM), southeast of Carletonville. Here, at about 880 m depth, the roughly north-south-trending Bank Fault is intersected in the vicinity of the MBF. Figure 3B schematically shows the geology along this crosscut. The breccia-rich zone is developed at the contact between Hospital Hill quartzite and Klipriviersberg lava. These generally well-separated formations are directly juxtaposed because of vertical displacement of 3500 m on the Bank Fault (cf. Fletcher and Reimold, 1989). The quartzite close to the breccia zone is transected by a syenitic dyke believed to be related to the Pilanesberg (1200 Ma) volcanic event. Except for a 2m-wide zone along the quartzite contact, where

### A Doornfontein G.M. (borehole)

Samples	1	Altered pseudotach.
	2	Quartzite (Roodepoort Argill. Qu.)
	3	Pseudotach.
	4	Quartzite (Footwall N Leader Qu.)
	5	Pseudotach.
	6	Dolomite (mylonite)
	7	Pseudotach. (after Black Reef shale)
	8	Pseudotach.
	9	Quartzite/Hanging-wall of Carbon Leader (R.L.C.)
	10	Ultramylonite
	11	Pseudotach.
	Deflection 1	Mylonitic quartzite (cut by pseudot.)
	12	(R.L.C. contact, equiv. sample 9)
	13	Altered dyke
	14	Pseudotach.
	Deflection 2	
	15	Pseudotach.

### B



### C

#### Bank Fault (Zone) East Driefontein G.M.

Schematic Section across 10m wide breccia zone,  
Borehole BOS7

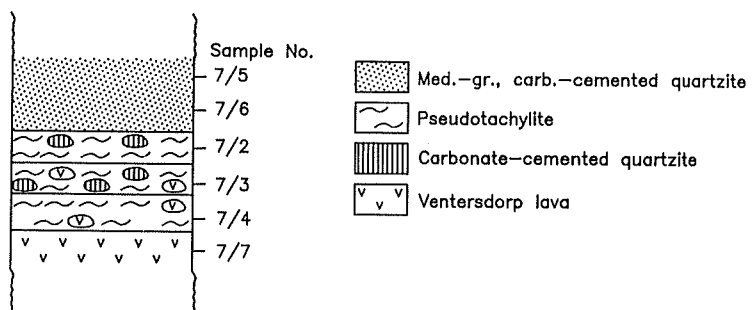


Figure 3: (A) Schematic lithostratigraphy apparent in the borehole section of drillcore BB18 (and two deflections) from Doornfontein Gold Mine. (B) Sketch of the geology at the Bank Fault breccia zone, East Driefontein Gold Mine, between Hospital Hill quartzite and Ventersdorp lava. (C) Section across the ca. 10 m wide breccia zone exposed in borehole BOS7

numerous meter-sized quartzite clasts are engulfed in pseudotachylitic matrix, the majority of the clasts in the breccia zone are lava-derived and range from a few centimeters up to a meter in size.

Sample 5A (Fig. 3B) from this section contains a quartz vein separating the lava clast from pseudotachylitic breccia. Detailed petrographic analysis (Fig. 4A) showed that this vein predates breccia formation and that, at least at this locality, only millimeter-wide movement took place in the breccia giving the impression of having been formed in a structurally turbulent environment. Most clasts, irrespective of their sizes, are well-rounded, apparently as the result of marginal melting rather than of turbulent flow and clast-clast milling action (however, this latter process is favoured for the origin of many cases of Vredefort breccias);

- (3) a few kilometers east of EDGM is Western Areas Gold Mine (WAGM), where Killick et al. (1988) collected a suite of samples from various stratigraphic levels in the Central Rand Group (Fig. 2), all close to important Kimberley reef horizons. Pseudotachylitic breccia G3 is hosted by Elsburg quartzite forming the footwall to the VCR; sample 36083A is hosted by Krugersdorp quartzite below the Kimberley Reefs in the Johannesburg Subgroup, and samples 36047 and G11 are hosted by Klipriviersberg lava close to the VCR, within phyllitic reef quartzite, near to the contact with footwall shale.

Killick et al. (1988) reported major element compositions for some of these samples and concluded that their breccia samples generally formed as mixtures of lava and metasediments, in various proportions. They also observed occasional enrichment in Cr and Pb in the breccias; and

- (4) the fourth suite of samples was obtained from drillcore BOS7 (Gold Fields of South Africa Ltd) from the Boskop Dam Project just east of the town of Potchefstroom. The 10m-wide breccia zone (Fig. 3C), containing on average about 8-m of pseudotachylitic breccia, occurs at about 3400 m depth between Ventersdorp lava and overlying quartzite, in a position that has been correlated with the MBF.

### Petrographic observations

Characteristic petrographic features of Witwatersrand pseudotachylitic breccias are summarised in Figures 4-8. Figure 4A demonstrates the typical layering between clasts and matrix. Figure 4B shows fine-grained devitrified pseudotachylite matrix, where the presence of microlites (compare Fig. 5E) proves the involvement of melting in the formation of this breccia. Other micropetrographic features that have been used to distinguish bona fide pseudotachylite from mylonitic or cataclastic breccias include (cf. also Maglaughlin and Spray, 1992b; Reimold and Colliston, 1994): the presence of vesicles in the matrix; corrosion textures at clast margins, considered to result from marginal melting; partial or complete assimilation of clasts by matrix resulting in "ghost clasts"; reaction or fusion rims around clasts; porous sinter textures in clasts; and sulphide droplets in the matrix.

Most of the samples used in the present study were derived from wide (several dm to m) breccia zones, such as the MBF, BRDZ, or VCR fault zones, and were identified as regular pseudotachylite. However, local variation between several fault rock types, over distances measurable in centimeters or decimeters, is characteristic of these fault zones.

*Figure 4: (A) View of a thin section across the contact between lava and pseudotachylitic breccia (arrows) in sample ED20/5A from EDGM. A ca. 0.5 cm wide quartz vein extends parallel to the contact. The light coloured clasts in the dark- and medium-grey, banded pseudotachylite are quartz clasts. Their texture suggests that they are derived from the quartz vein (compare Fig. 6E). Light grey clasts surrounded by darker pseudotachylite are lava fragments. Scale bar = 0.3 cm. (B) Fine-grained, devitrified pseudotachylite BOS7/3. Lath-shaped microlites are plagioclase, needle-shaped crystals are secondary sericite that in places occur as spherulitic patches. Crossed polarizers, width of field of view = 650 µm. (C) Dense, clast-poor pseudotachylite from level 22 in EDGM. This sample contains up to 9cm-long and 3cm-wide oblong amygdalules filled mainly with quartz and minor calcite. The vesicles are irregularly oriented and a few roundish, chlorite-filled microvesicles are present in the matrix (arrow). (D) Thin section of pseudotachylite (1), PU-15A with large clasts of shale (2), and an older, altered ultramylonite (3). Scale bar = 0.3 cm. (E) Part of a 1cm-wide clast of coarse-grained quartzite with planar fluid inclusion trails in pseudotachylite BOS7/5 (compare Leroux et al., 1994). Note that these trails cut across a series of primary fluid inclusion bands. Crossed polarizers; width: 1.1 mm*

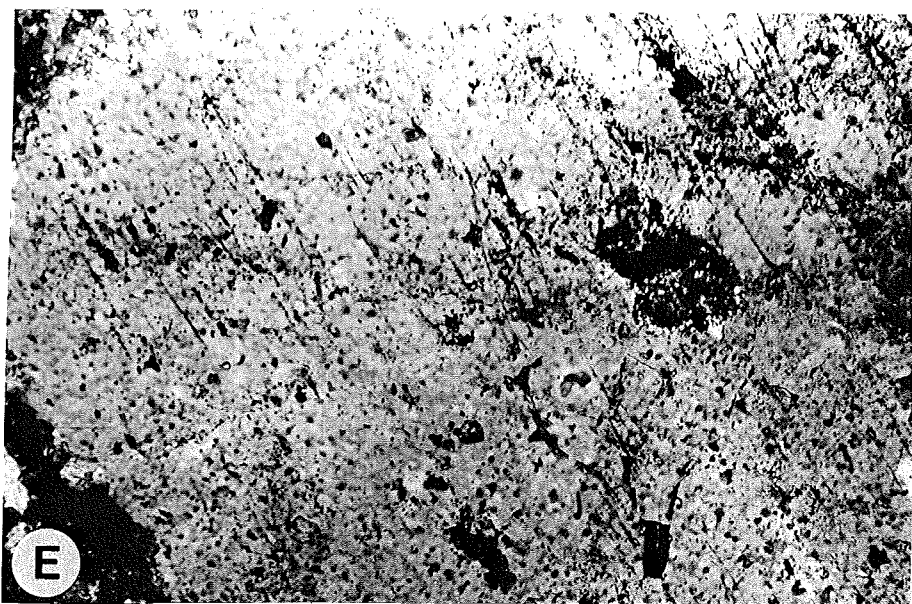
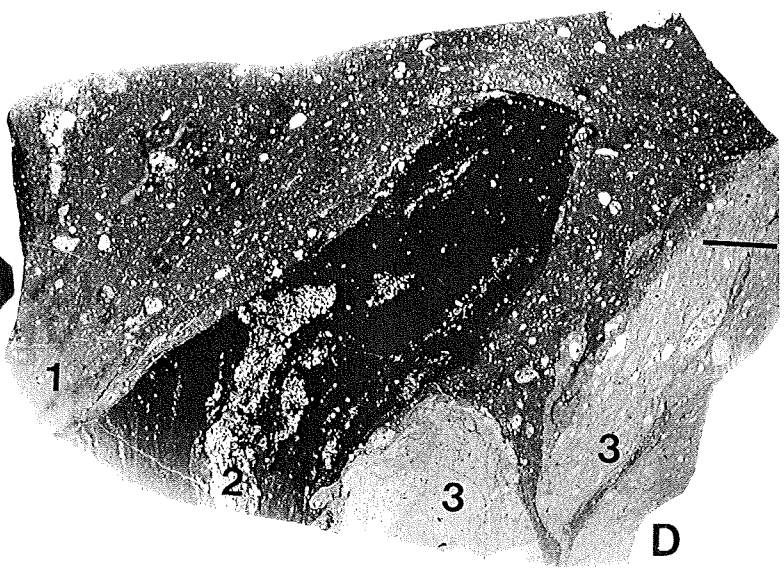
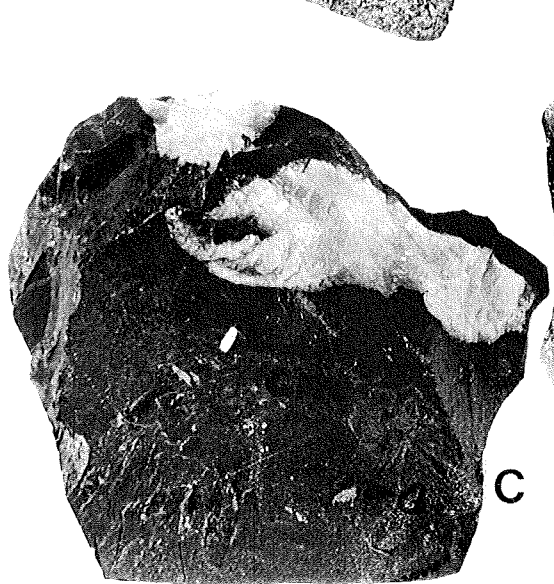
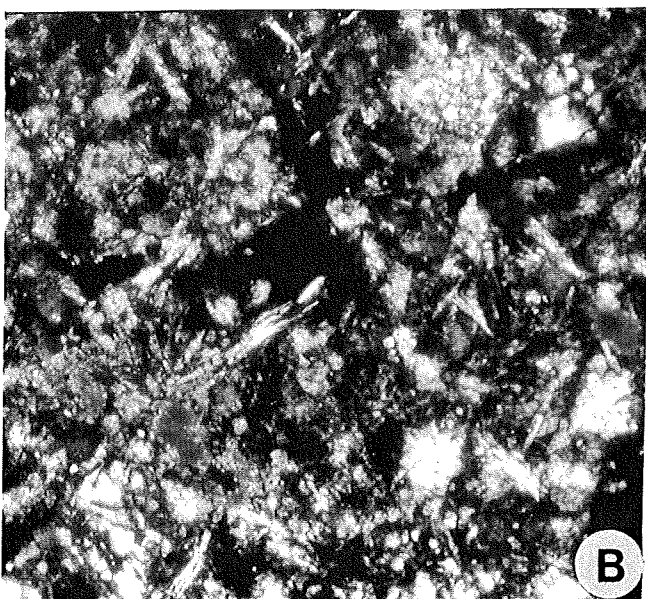
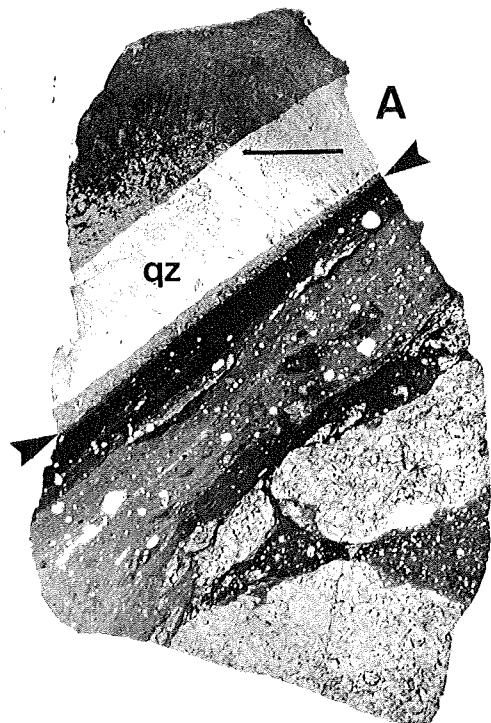


Figure 4C represents a dense, aphanitic, and clast-poor pseudotachylite from EDGM. It contains a number of large quartz- and quartz-carbonate-filled vesicles. Such vesicles are also abundant on the micro-scale. This observation, together with vesicle-filling minerals intimately intergrown with matrix microlites (some of which may be altered), indicates that autometasomatism occurred during pseudotachylite formation.

Both Vredefort and Witwatersrand pseudotachylitic breccias commonly show evidence for multiple breccia generation. Figure 4D shows a younger pseudotachylite (1) containing shale clasts (2) and an older generation of breccia (3). Other examples of breccia-in-breccia development are shown in Figures 5C and 7B. (Sub)planar microdeformation features also occur in quartz clasts in both Vredefort and Witwatersrand breccias (Fig. 4E). This deformation phenomenon is, however, more frequently observed in Vredefort samples (compare Reimold, 1990; Grieve et al., 1990; Hart et al., 1991; Leroux et al., 1994).

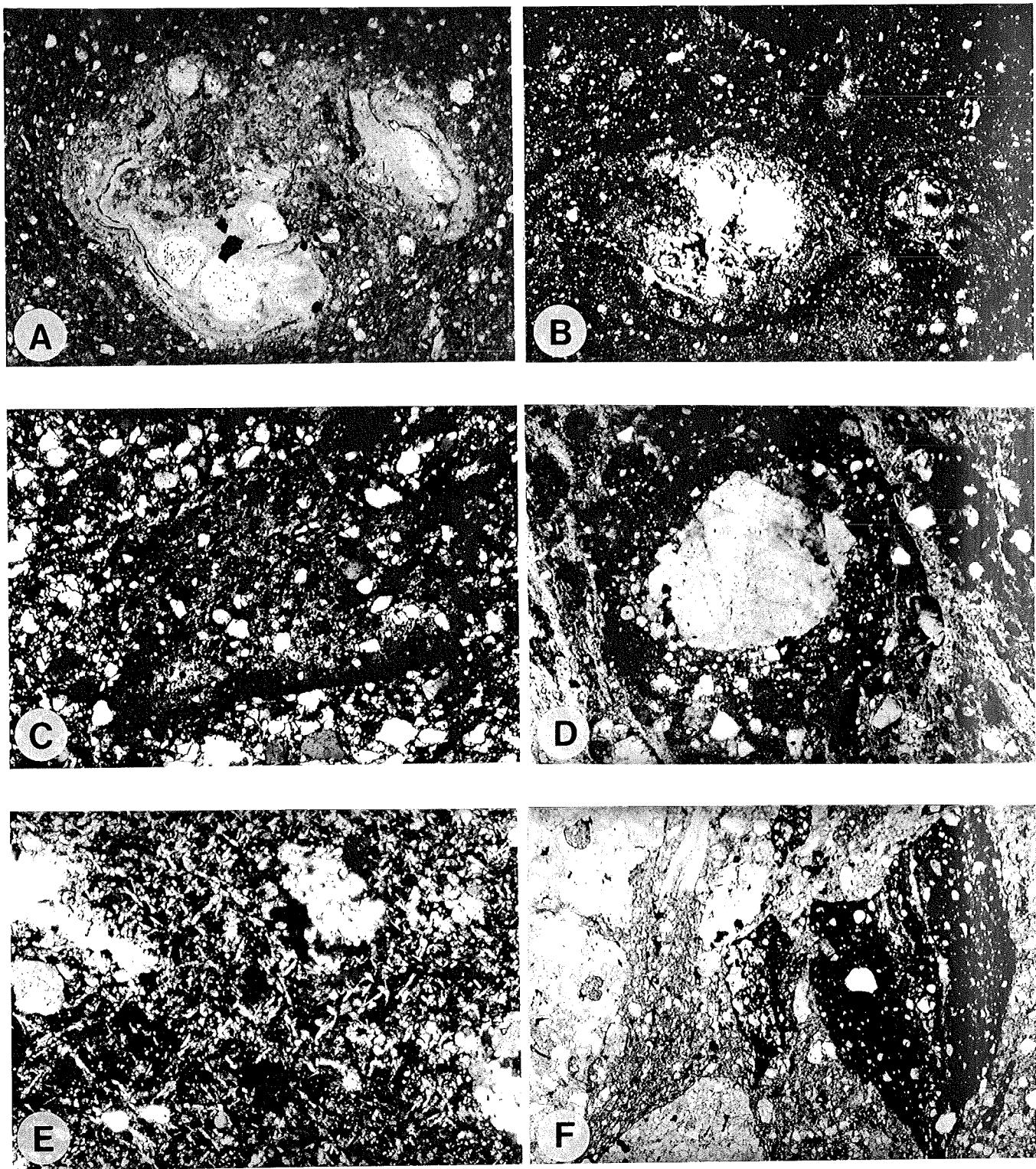
Figures 5A,B,D and F illustrate typical clast appearances. With the exception of refractory quartz (Spray, 1992) and mature quartzite clasts, most other clast lithologies (lava, shale, sericitic- or carbonate-rich quartzite, etc.) are either partially (Fig. 5D) or completely (Fig. 8D) annealed or melted in pseudotachylite and are usually only recognisable as "ghosts". This is generally not the case for clasts in cataclasites. In addition, the ratio of angular-to-rounded clasts is much higher in cataclasites.

Typical examples of micro-vesicles in pseudotachylites are shown in Figures 6A-D and 8B and C. Vesicles may be filled with quartz, chlorite, pyrite or pyrrhotite or calcite, or combinations of all these minerals, either in the form of intergrowths, or being zoned in no characteristic sequence. A quartz rim surrounding an opaque phase (mainly pyrite or pyrrhotite, but also including sphalerite and minor rutile and galena) is commonly observed and is consistent with the crystallisation temperatures for these minerals.

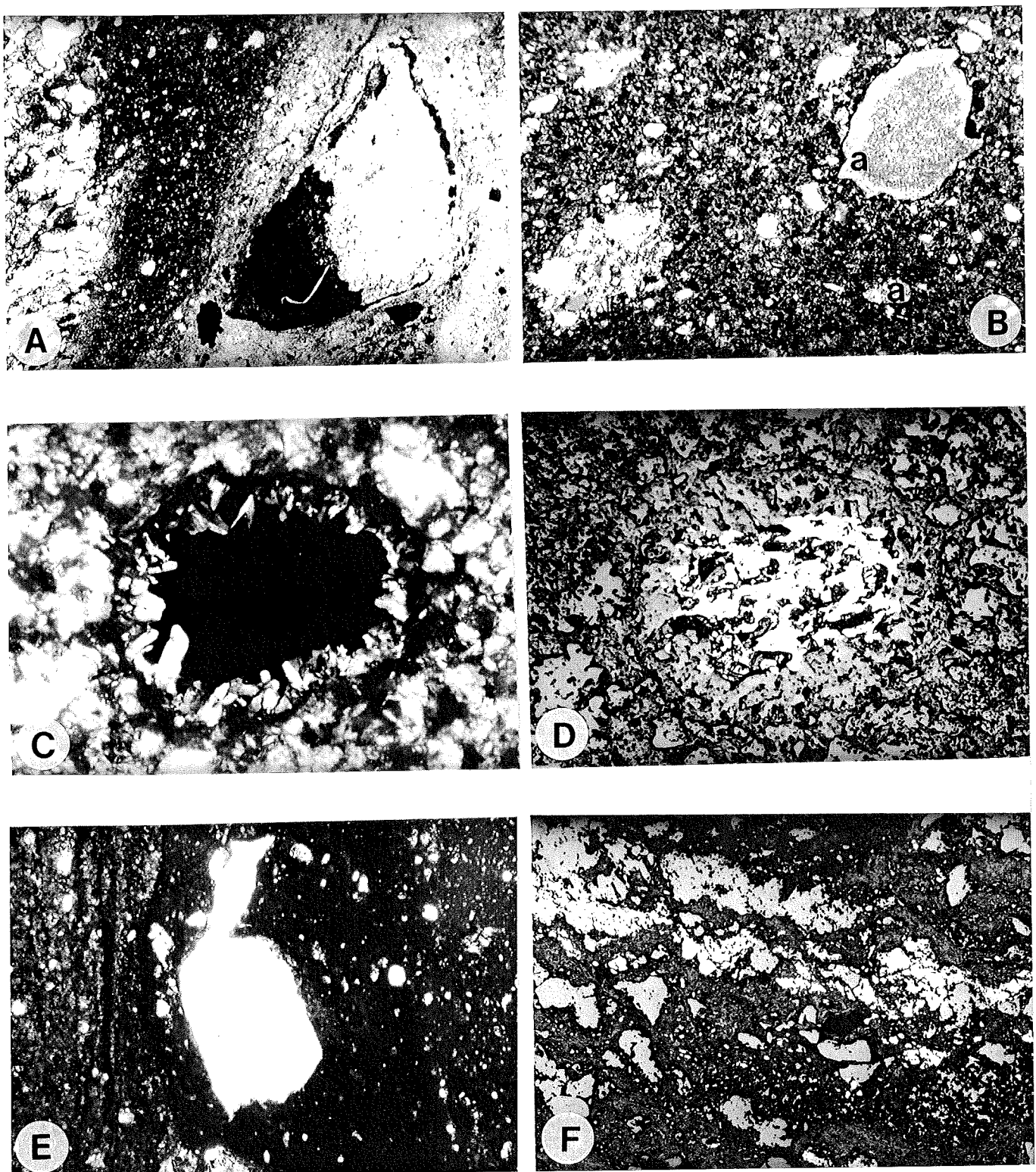
It is evident from Figure 6F that, while secondary hydrothermal sulphide growths are abundant in the fault rock matrices, primary sulphide is also present and can often be recognized texturally: such grains may be strongly fractured or even brecciated (as in Fig. 6F - also indicating limited lateral movement), or they may be well-aligned with flow structures in the matrix, or show marginal melting (see also Figs. 7C-E, F and I). Figures 7A and E, and Figure 8A, demonstrate, however, that hydrothermal activity in the Witwatersrand Basin did not only take place at the time of breccia formation, but also occurred at various other stages in the evolution of the Basin. Pre- and post-breccia formation quartz and quartz-carbonate veins are commonly observed.

Figure 7I provides an example of wall-rock alteration along pseudotachylitic breccia veins, frequently observed along breccia-bearing faults in the Basin as well as in the Vredefort Dome.

In conclusion, field and petrographic evidence demonstrate that autometasomatism took place during breccia generation (as emphasized by the vesicle record, presence of quartz- and quartz-carbonate-filled veinlets between fault breccia and wallrock - without any evidence of tectonic movement). In addition, brecciation was followed by alteration and some tectonic disturbance.

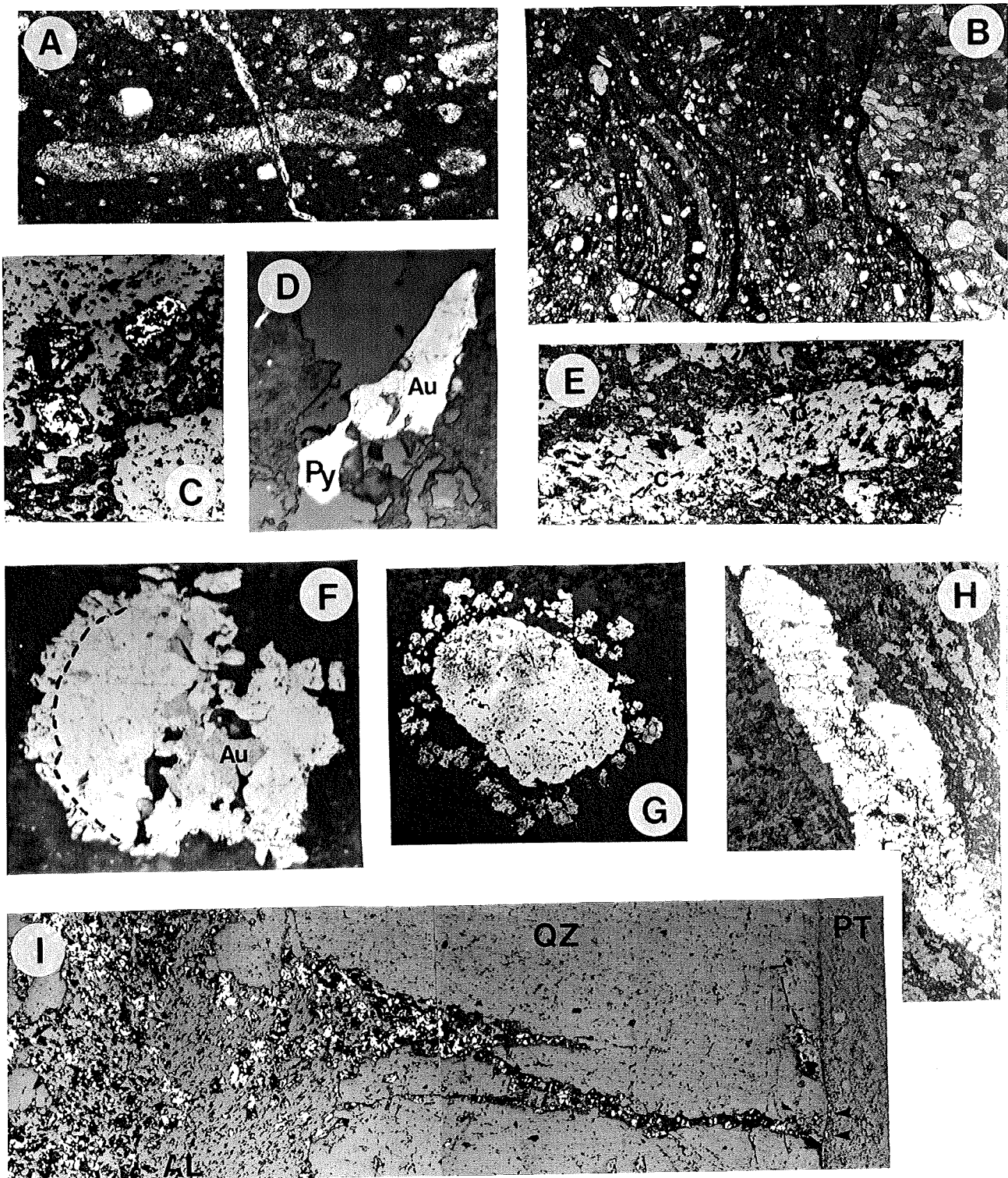


*Figure 5: (A) Pseudotachylite sample 36083 (WAGM): a partially-melted quartzite clast (opaque phase = pyrite); parallel polarizers, 2.2 mm wide. (B) Example of two largely matrix-assimilated quartzitic clasts. The remaining clasts are strongly annealed. Crossed polarizers, 3.4 mm wide. (C) Fragment of older pseudotachylitic breccia with chloritized matrix set in cataclasite of sample G11A from Western Areas. Crossed polarizers, 1.1 mm wide. (D) "Ghost" clast (dark halo around large quartz grain in centre) - relic of a largely melted quartzite fragment, set in partially altered (lighter schlieren) pseudotachylite. Parallel polarizers, 2.2 mm wide. (E) Microcrystalline (plagioclase laths - partially sericitized) matrix to pseudotachylite BOS7/4. Crossed polarizers, 1.4 mm wide. (F) Pseudotachylite PU-12A with light quartzite and two dark shale clasts in medium-grey matrix. Contact with host quartzite on left margin (note embayments and fracture fillings of melt). Parallel polarizers, 3.4 mm wide.*



**Figure 6:** (A) Pseudotachylite BOS7/3: Chlorite (dark) and calcite-filled vesicle near contact between breccia and quartzitic host rock. Quartzite is slightly sheared. Crossed polarizers, 2.2 mm wide. (B) Two carbonate-filled amygdalites (a) in pseudotachylite PU-11. Also shown are several partially melted quartzite clasts and a few microlites in the matrix. Crossed polarizers, 3.4 mm wide. (C) Quartz/pyrite (dark)-filled vesicle in pseudotachylite PU-3. Crossed polarizers, 0.9 mm wide. (D) The same as (C), but in reflected light. (E) Pseudotachylite near the contact with the quartz seam shown in Fig. 4A, illustrating a large inclusion of vein quartz which is obviously older than the breccia. Note the narrow, lighter coloured halo of partially assimilated material around the clast. Crossed polarizers, 2.2 mm wide. (F) A trail of partially brecciated pyrite crystals in ultramylonite ED-20/17. Such pyrite grains were not identified in the host rock, but may have been introduced during lateral mixing. Reflected light, 1.1 mm wide.

*Figure 7: (A) Pseudotachylite PU-10 (Doornfontein G.M.). Evidence for two stages of hydrothermal activity: calcite-filled vesicles formed at the time of pseudotachylite formation are cut and displaced by a later carbonate-filled joint. Crossed polarizers, 3.4 mm wide. (B) Pseudotachylite PU-12A, containing a clast of older pseudotachylite (left, margin enhanced by solid line) as well as older quartzitic cataclasite. Width: 3.4 mm. (C) Pseudotachylite PU-4 with three euhedral Au grains in a quartz clast. Width: 430 µm. (D) Quartzitic clast in pseudotachylitic breccia PU-12B: a gold grain in paragenesis with pyrite (Py) and surrounded by quartz. Width: 590 µm. (E) Pseudotachylite PU-5 cut by a calcite vein (light grey, trending SW-NE) carrying several pyrite (p) and chalcopyrite (c) grains. Width: 800 µm. (F) Pseudotachylite BOS7/2: euhedral gold in detrital pyrite that, in turn, is overgrown by spongy secondary pyrite (enhanced by dashed line). Width: 165 µm. (G) Pseudotachylite ED-20/14A: well-rounded detrital pyrite grain showing marginal resorption; it served as a nucleus for the crystallization of small euhedral pyrite crystals from the pseudotachylitic matrix. Width: 700 µm. (H) Quartzitic host rock to pseudotachylite BOS7/4: cataclastic pyrite in shear band parallel to contact with pseudotachylite; longer side is 1 mm wide. (I) Profile across pseudotachylite (PT), quartz vein (QZ) along host rock-pseudotachylite contact, and altered host rock, Ventersdorp lava. Note minor secondary pyrite growth in pseudotachylite; significant pyrite deposition took place in fractures through the quartz vein and is disseminated throughout altered lava. Width: 6.2 mm. (Photographs (A) and (B) were taken with parallel polarizers, all others are reflected light images).*



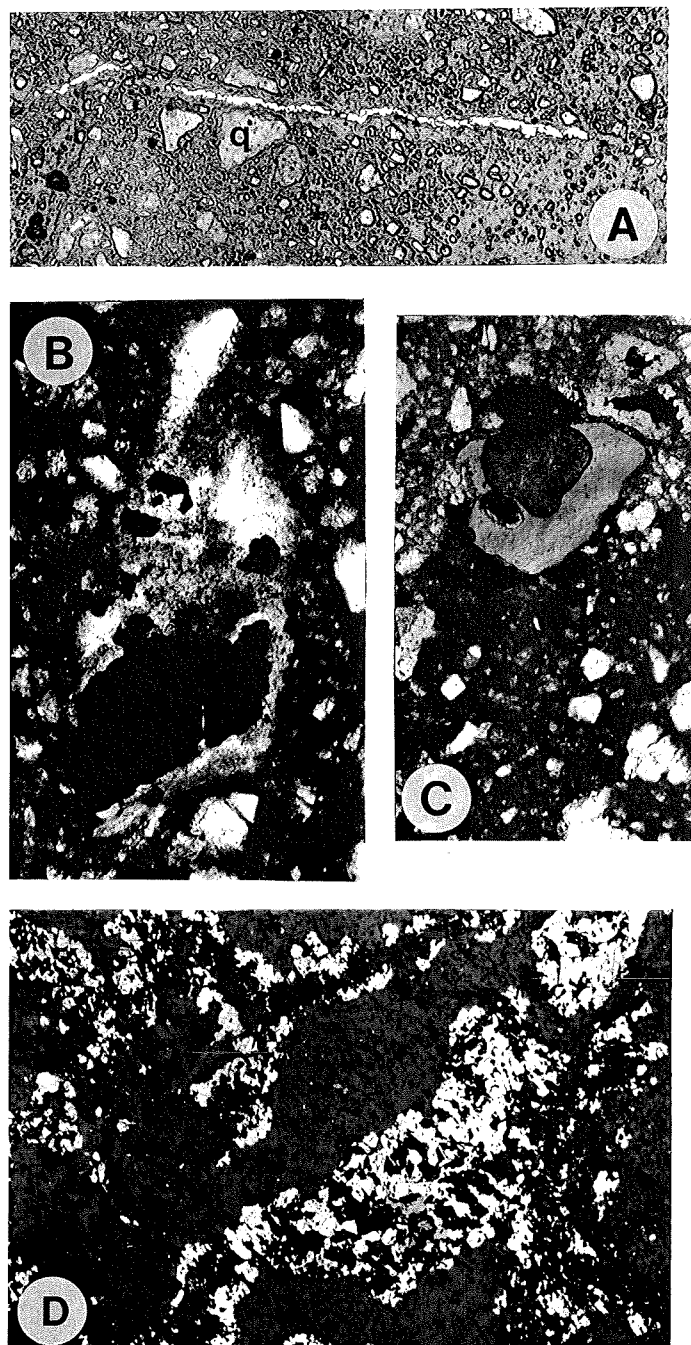


*Figure 8: (A) Pseudotachylite 69257A (WAGM): secondary pyrite precipitated along fracture across breccia. Note brecciated quartz clast (Q) transected by joint. Reflected light, 1.1 mm wide. (B) Sample G11 (WAGM): chlorite-filled vesicle with pyrrhotite (black) in pseudotachylite. Parallel polarizers, 1 mm wide. (C) Cataclastic quartzite clast (upper half) at contact with pseudotachylite G11 (dark matrix); chlorite-filled vesicle at contact, rimmed by pyrrhotite; quartz fragments contain marginally corroded pyrite. Parallel polarizers, 1.75 mm wide. (D) Completely annealed quartzite clast in pseudotachylite G11. Matrix contains secondary chlorite (dark grey against pyrrhotite) and remelted pyrrhotite (symplectite). Reflected light, 1.1 mm wide.*

## Experimental procedures

Major and trace element data are presented in Tables 1-4. East Driefontein data (Table 1) were obtained by XRF analysis at Gold Fields Laboratories (Pty) Limited in Johannesburg. XRF data for Doornfontein samples were obtained through Bergström and Bakker Laboratories, Johannesburg. Some XRF major and trace element data for Western Areas samples were previously reported by Killick et al. (1988). The remaining samples from this suite were analysed by XRF in the Department of Geology, University of the Witwatersrand. Concentrations for thirty-two trace elements were determined by instrumental neutron activation analysis (INAA) at the Institute of Geochemistry, University of Vienna, according to methods described by Koeberl et al. (1987). Samples from borehole BOS7 were also analysed by INAA in Vienna. XRF data for this sample suite were generated at the Council for Geosciences in Pretoria.

## Results

### *1. East Driefontein Section*

The analytical data for the EDGM samples are shown in Figures 9A and B. A first-order observation is a strong depletion for all elements, except  $\text{SiO}_2$  and  $\text{K}_2\text{O}$ , across the fault zone. Pseudotachylite samples show some degree of compositional similarity to the host rock lithology that is dominant in a specific sampling area: in the broad breccia zone between samples 13 and 7, pseudotachylite resembles lava 7, whereas breccias 16 and 14A, collected in quartzite, represent mixtures of quartzite and lava. The  $\text{Na}_2\text{O}$  profile displays some anomalies (e.g., samples 14A and 11), which could be explained either as a local mixing effect (variable clast/breccia ratios) or as the result of hydrothermal alteration. The consistent depletion of major and trace elements determined for samples 17 and 13 near the contact quartzite-breccia zone is a result of silicification, as evidenced by the sympathetic increase in  $\text{SiO}_2$  contents and the presence of quartz veining mentioned earlier. Figure 5E showed that these quartz veins partially pre-date pseudotachylite formation and that the effect of silicification is not a pervasive feature of this fault zone.

In the trace element plot (Fig. 9B), concentration levels are generally not very different for the two precursor rock components. Thus, these data do not permit any conclusions regarding mixing during pseudotachylite formation. Zn is a notable exception, but this element is not only heterogeneously distributed in the quartzite, but significant amounts of sphalerite have been observed in many Witwatersrand fault zones and strata. Sphalerite is generally part of a secondary paragenesis (with galena, chalcopyrite, pyrite or pyrrhotite) in hydrothermal veins or in the matrices of fault breccias. It is, therefore, not possible to determine how much Zn has been introduced with secondary fluids or remobilised from primary lithologies. Trace elements are also somewhat depleted along the margin of the fault zone.

### *2. Doornfontein Drillcore*

The Doornfontein data (Table 2, Fig. 10) must be considered against the complex borehole stratigraphy (Fig. 3A). Radically changing compositions from sample to sample only permitted major element data to be presented in profile form. Chemical compositions highlight two unique lithologies, a dolomite clast and a mafic dyke. Comparison between the chemistry of these two

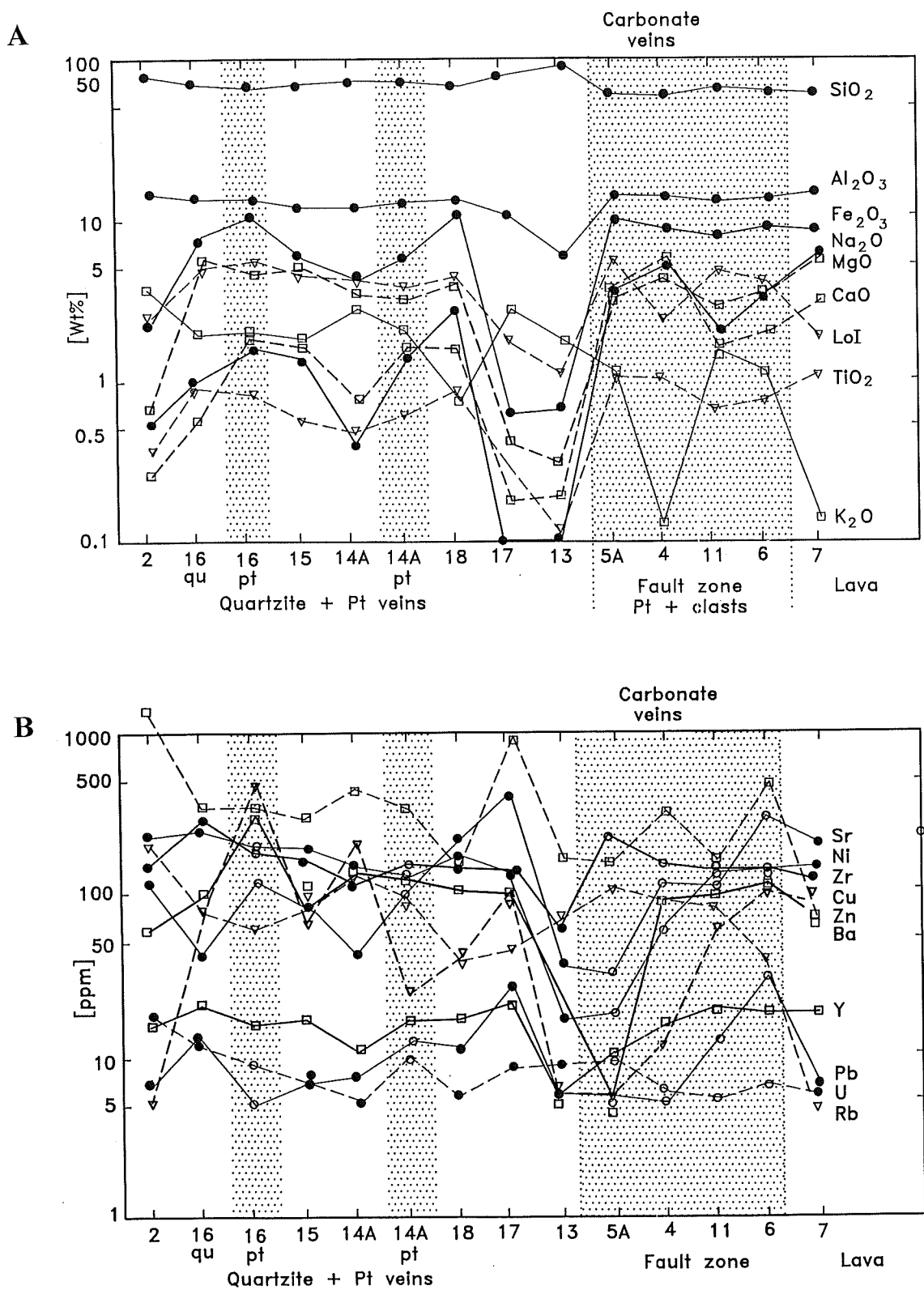


Figure 9: Major (A) and trace element (B) profiles across the Bank Fault intersection on East Driefontein Gold Mine.

**Table 1 : Major ( wt% ) and trace element (ppm) compositions, by XRF, of samples from the East Driefontein Gold Mine traverse. Data obtained from Gold Fields Laboratories (Pty) Ltd. \* Total Fe as  $\text{Fe}_2\text{O}_3$**

Sample	ED-2 Quart.	ED-16Q Quart.	ED-16PT Pseudt.	ED-15 Q./PT	ED-14AQ Quart.	ED-14APT Pseudt.	ED-18 Pseudt.	ED-17 Quart.	ED-13 Pseudt.	ED-5A Pseudt.	ED-4 Lava	ED-11 Pseudt.	ED-6 Pseudt.	ED-7 Lava
Si <sub>02</sub>	76.25	64.80	61.13	68.40	73.12	69.11	59.54	84.42	90.74	56.22	57.39	65.00	62.72	58.70
Ti <sub>02</sub>	.32	1.00	.84	.57	.46	.62	.89	.28	.11	1.09	1.02	.65	.77	1.05
Al <sub>2</sub> O <sub>3</sub>	14.20	12.43	13.31	11.77	11.78	12.83	13.77	10.23	5.60	14.47	14.25	12.82	13.13	14.50
Fe <sub>2</sub> O <sub>3</sub> *	2.38	7.62	9.71	5.29	4.02	5.70	11.21	.63	.67	10.21	8.83	7.76	8.90	8.29
Mn <sub>0</sub>	.01	.12	.15	.10	.06	.10	.12	.01	.01	.16	.11	.06	.13	.11
Mg <sub>0</sub>	.58	5.13	4.72	4.58	3.26	3.22	4.23	.36	.28	3.25	4.45	2.76	3.41	5.69
Ca <sub>0</sub>	.15	.93	1.76	1.60	.69	1.58	1.55	.18	.19	3.94	6.46	1.63	1.89	3.26
Na <sub>2</sub> O	.56	1.45	1.68	1.35	.38	1.40	2.85	.06	.10	3.55	5.68	1.92	3.73	6.01
K <sub>2</sub> O	3.55	1.90	1.41	1.73	2.82	1.97	.71	2.84	1.79	1.09	.13	1.55	1.09	.14
P <sub>2</sub> O <sub>5</sub>	.02	.06	.14	.04	.02	.14	.24	.01	.01	.23	.14	.19	.21	.15
Lo <sub>1</sub>	2.30	4.87	5.70	4.34	4.04	3.66	4.49	1.67	1.12	5.37	2.41	4.93	3.86	1.83
Total	100.32	100.31	100.55	99.77	100.65	100.33	99.60	100.69	100.62	99.58	100.87	99.27	99.84	99.73
Ni	214	245	195	195	142	122	156	130	15	17	60	130	137	136
Cu	5	88	485	64	196	23	39	99	5	5	12	55	103	82
Pb	6	12	5	6	7	12	11	26	5	5	5	48	29	6
Zn	48	91	315	76	146	113	101	95	5	5	86	91	118	72
Rb	195	78	57	73	123	90	38	42	65	101	82	76	36	5
Sr	115	43	123	72	40	99	213	405	34	29	107	106	286	177
Ba	1469	332	352	257	481	156	136	914	157	146	325	142	462	59
Y	16	20	15	16	10	16	20	5	10	14	18	17	17	17
Zr	148	297	186	165	119	151	131	132	59	216	148	130	137	107
U	18	11	9	6	5	10	5	8	8	9	6	5	6	5

rocks and those of adjacent breccia samples show that the dyke slightly affected the surrounding matrix, whereas no evidence of mixing of the dolomite with the breccia is evident. Pseudotachylite and mylonite samples all have similar compositions, with the exception of sample PU-1 which is strongly altered (high K<sub>2</sub>O resulting from sericitisation). Thus, it appears that the massive breccia at this MBF intersection is well homogenised. Some variability is detected for MgO, but this could be the result of local chloritisation of the breccia matrix.

The breccia zone is also homogeneous with regard to trace elements, at least within the constraints set by the primary heterogeneity of the country rocks (cf. compositions of quartzites PU-2, -4, -9, and -12). Altered pseudotachylite PU-1 is anomalous, with enrichments of Ba, Rb, and Sr, and depletion of Co. Three samples (PU-3, -7, and -15) are strongly depleted in U compared to the remaining samples. However, as this effect is not accompanied by other element variations, this could well be a primary mineralogical phenomenon (heterogeneous distribution of uraninite in precursor rock) rather than evidence for hydrothermal overprinting.

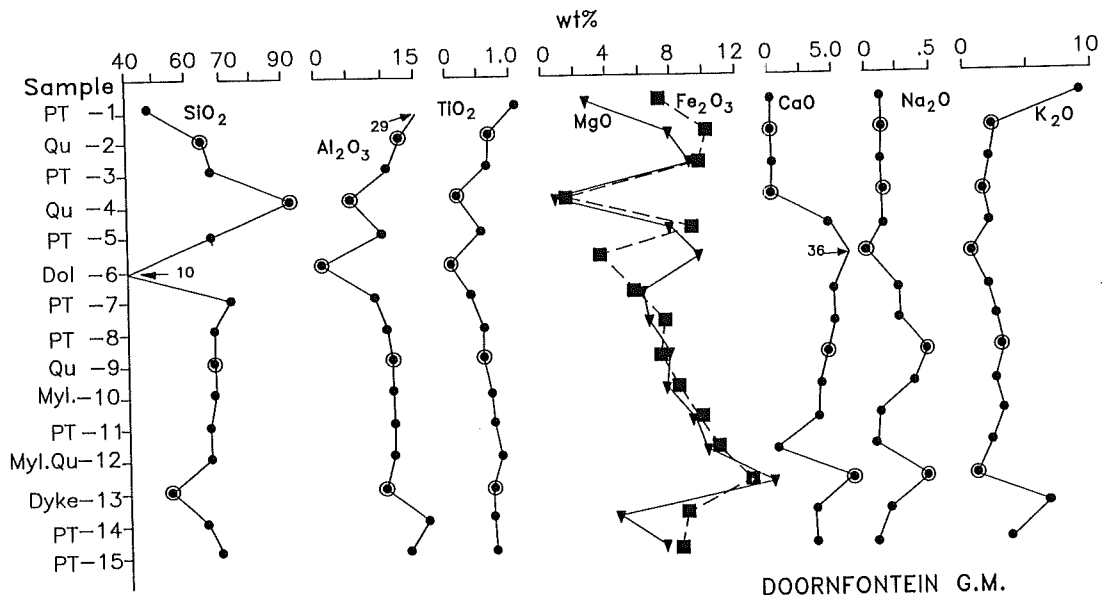


*Figure 10: Major element profiles across the borehole intersection of the Master Bedding Fault on Doornfontein Gold Mine.*

### 3. Western Areas Suite

#### (a) Major element systematics

Isocon diagrams (Fig. 11) for the Western Areas data (Tables 3A and B) illustrate the major element systematics between individual pseudotachylite-host rock pairs. Data were plotted prior to correction for volatile contents ranging from 1.35 to 8.1 wt%, as all samples had been affected by alteration.

**Table 2 : Compositions of lithologies from borehole BB18, northeast sector of Doornfontein Gold Mine. XRF data, analysts : Bergström and Bakker Laboratories, Johannesburg. Major element results recalculated to 100 wt%; trace element data in ppm; \* $\text{Fe}_2\text{O}_3$  = total Fe; bd = below detection limit; nd = not determined**

Sample	PU-1 Pseudt.	PU-2 Quart. Pseudt.	PU-3 Quart. Pseudt.	PU-4 Quart. Pseudt.	PU-5 Pseudt.	PU-6 Dolom. Pseudt.	PU-7 Shale Pseudt.	PU-8 Quart. Pseudt.	PU-9 Quart. Pseudt.	PU-10 Shale Pseudt.	PU-11 Pseudt.	PU-12 Pseudt.	PU-13 alt.dyke shale	PU-14 shale	PU-15 Pseudt.
SiO <sub>2</sub>	48.30	64.40	66.60	91.00	10.26	72.20	67.91	66.50	66.30	64.90	64.80	53.30	63.90	68.10	
TiO <sub>2</sub>	1.07	.64	.57	.08	.51	.03	.34	.49	.46	.55	.58	.59	.60	.62	
Al <sub>2</sub> O <sub>3</sub>	29.10	12.70	10.40	5.10	9.94	1.05	8.30	9.88	10.70	11.00	10.40	9.90	16.00	12.60	
Fe <sub>2</sub> O <sub>3</sub> *	7.30	10.10	9.60	1.17	8.14	3.30	5.65	7.16	6.96	8.00	8.30	10.45	12.70	8.50	
MnO	.03	.10	.12	bd	.25	1.95	.26	.27	.15	.20	.21	.16	.23	.05	.12
MgO	2.60	7.80	9.00	.50	7.96	9.26	6.02	6.47	7.00	7.30	8.40	9.70	13.90	4.24	7.04
CaO	.15	.10	.15	.11	4.00	36.10	4.43	4.68	3.87	3.43	3.16	.08	6.70	.36	.15
Na <sub>2</sub> O	.10	.13	.10	.05	.13	.01	.17	.22	.35	.25	.04	.01	.44	.08	bd
K <sub>2</sub> O	9.01	2.17	1.70	1.03	1.74	.16	1.47	1.91	2.36	2.03	2.17	1.38	.10	5.74	2.81
P <sub>2</sub> O <sub>5</sub>	.03	.03	.04	.01	.04	.03	.05	.03	.04	.04	.03	.04	.04	.06	.06
S	.62	.04	.10	.03	.04	.31	.03	.04	.04	.06	.05	.04	.04	.07	.07
Sc	4	bd	4	bd	1	3	1	3	bd	4	4	3	4	4	1
Co	3	12	25	bd	23	4	20	38	28	29	40	46	56	32	25
Ni	100	215	159	34	13.4	15	76	143	164	136	148	273	207	104	159
Cuu	95	47	53	61	81	22	25	63	61	52	41	47	46	69	70
Zn	32	87	202	35	65	21	40	86	63	58	77	108	86	44	185
Ga	36	16	21	4	15	1	5	9	9	18	12	13	16	22	18
Rb	20.8	57	62	36	66	bd	44	76	79	71	66	46	7	180	82
Sr	43	nd	2	6	26	185	43	106	52	50	52	1	177	31	14
Nb	1.8	3	7	1	7	5	5	10	8	7	7	3	6	3	9
Zr	15.8	92	152	98	158	16	94	154	104	146	155	110	55	91	120
Y	4.6	16	11	7	25	12	9	17	20	21	16	17	12	25	25
Ba	89.0	34.2	19.3	14.8	18.2	56	140	102	235	200	201	260	130	314	280
La	37	22	16	51	26	6	13	20	22	25	45	10	19	25	23
Ce	9.2	5.1	4.4	2.1	24	13	44	35	29	18	77	5	4	19	35
Th	8	nd	nd	9	nd	1	28	13	16	2	26	11	nd	11	11
U	5	1	bd	1	8	8	bd	4	1	9	10	11	21	5	bd

For the 36083 samples (Fig. 11A), SiO<sub>2</sub> is strongly depleted in the pseudotachylite and is naturally accompanied by enrichment of all other elements except Na<sub>2</sub>O. Killick et al. (1988) considered such a relationship as possible evidence for mixing of the quartzitic host rock component with mafic lava. However, considering the high volatile content of the fault breccia and the enrichment of K<sub>2</sub>O, it is possible that alteration is a likely cause of these chemical relationships. The depletion in SiO<sub>2</sub> could, thus, be an effect of (1) alteration (introduction of volatile phases, increase of K<sub>2</sub>O) or of (2) admixture of a mafic component (shale or lava) that might have been more susceptible to melting than the refractory quartzite. In addition, this could explain the considerable increase in Fe and Mg contents in the breccia. However, the petrographic study showed that the breccia contains numerous chlorite-filled vesicles, whereas the clast population contains an overwhelming proportion of quartz and quartzite, with only a minor shale and siltstone component.

Pseudotachylite sample 49006A was hosted by shale (49006C) and mafic phyllite (49006B) (Fig. 11B, Table 3A). The development of pseudotachylite as a mixture of both country rock types appears realistic with regard to most major elements. Ca and the alkali elements do not, however, conform with such a mixing model (K<sub>2</sub>O depleted, Na<sub>2</sub>O and CaO too high). Alteration is the more likely process to have affected the concentrations of the more mobile elements, but the normally expected alteration trends that would normally be expected (increasing K and decreasing Ca and Na) are not observed. In the absence of any other plausible explanation, our preferred hypothesis to explain the elemental behaviour is mixing, but mixing of two internally heterogeneous components for which the available analyses may not be representative.

**Table 3A :** Major element data ( by XRF, in wt %) for selected pseudotachylite-host rock pairs from Western Areas Gold Mine ( bd = below detection limit; \* Fe<sub>2</sub>O<sub>3</sub> = total Fe )

Sample	49006A Pseudt.	49006B Phyll.	49006C Shale	62957A Pseudt.	62957B Quartz.
SiO <sub>2</sub>	60.31	51.22	74.47	69.09	90.34
TiO <sub>2</sub>	.66	.80	.38	.91	.10
Al <sub>2</sub> O <sub>3</sub>	20.41	23.24	17.83	21.17	5.00
Fe <sub>2</sub> O <sub>3</sub>	4.48	6.70	.24	.90	2.00
MnO	.05	.06	.01	bd	bd
MgO	3.45	6.90	.25	.32	.08
CaO	.30	.27	.13	.34	.13
Na <sub>2</sub> O	1.33	1.14	.87	1.91	.57
K <sub>2</sub> O	2.93	2.96	3.55	1.80	.38
P <sub>2</sub> O <sub>5</sub>	.09	.10	.04	.05	.02
Lo I	6.03	7.62	2.44	4.81	1.12
Total	100.04	101.01	100.21	100.30	99.74

**Table 3B :** Trace element contents in selected pseudotachylite-host rock pairs from Western Areas Gold Mine. INAA data, in ppm, but Au in pbb. Analyst : C. Koeberl, Vienna. For XRF major element data of these samples, cf. Killick et al. ( 1988 )

Sample	36083A Pseudt. Quartz.	36083B Pseudt. Quartz.	49006A Pseudt. Phyll.	49006B Shale	49006C Pseudt. Quartz.	G3 Pseudt. Quartz.	G4 Pseudt. Quartz.	62957A Quartz. Pseudt.	62957B Quartz. Pseudt.	36047 Pseudt. Lava	36044 Pseudt. Lava	611 Pseudt. Lava	65 Pseudt. Lava
Sc	24.6	5.38	22.1	24.2	8.28	16.1	3.01	11.6	2.99	17.3	41.5	10.7	25.7
Cr	535	120	680	960	180	590	61	320	100	290	150	.790	2400
Co	58.2	13.4	46.5	52.4	3.91	51.8	6.62	40	23.4	49	82.6	75.7	268
Ni	348	<50	430	304	23	500	4.7	130	50	180	100	850	3100
Zn	124	26.9	97	190	<2	740	28.6	28	7	130	900	205	257
Ga	92	18	4.4	60	19	18	8.9	24	45	10.3	17.7	27	17.9
As	44.2	25	97	65	9.54	3.01	53.9	143	49	4.09	17.8	2.14	515
Se	1.2	.8	2.1	1.6	.9	<1	.5	.6	.8	<1	2	.7	1.3
Br	.4	.32	<1	.3	<.4	<.3	<.1	<.4	.773	<.3	<.4	.24	<.4
Rb	114	68	140	133	121	74.5	.58	57.2	11.9	46.8	<12	6.8	7.2
Sr	<80	<35	67	96	<100	<28	140	125	100	80	40	<50	
Zr	240	140	25.0	190	100	170	61	220	140	150	230	112	85
Ag	<.4	<.6	2.3	<.8	.2	<1	<.5	<.8	<.5	<1	.1	<1	
Sb	2.21	.98	3.97	.61	.46	.62	.34	4.34	.96	.41	.64	.97	1.13
Cs	6.1	2.17	69.5	6.76	6.48	1.47	1.27	8.34	1.04	2.7	.70	.96	.98
Ba	150	90	180	220	250	160	6.0	80	<100	40	40	20	
La	20.7	34.2	88.6	9.85	30.5	20.5	12.4	11.4	19.8	15.3	12.7	16.4	4.89
Ce	44.6	59.2	154	21	52.3	43	20.7	22.4	15	34.4	46.4	35.8	13.9
Nd	22.1	24.9	66.3	12.7	20.6	20.9	7.54	12.4	15	16.6	31.4	16.7	6.9
Sm	4.9	3.92	10.7	3.08	2.79	4.71	1.35	3.24	2.44	3.85	8.12	3.71	2.03
Eu	1.05	.94	2.5	.68	.70	1.09	.21	.76	.5	1.4	3.32	.83	.64
Gd	4.6	2.2	7.3	3.7	3	5.6	1.7	3.3	1.7	4.1	9.8	2.9	2.7
Tb	.82	.40	1.32	.68	.56	1.03	.31	.58	.3	.75	1.72	.5	.5
Dy	5.1	2.1	7.6	3.4	3	5.7	1.9	3.6	1.7	4.2	10.3	2.9	3.2
Tm	.45	.13	.54	.24	.17	.35	.17	.32	.11	.3	.84	-	.3
Yb	2.74	.7	2.66	1.12	.64	1.65	1.09	1.8	.7	1.49	4.43	.92	1.97
Lu	.39	.13	.375	.17	.096	.26	.16	.27	.11	.22	.61	.14	.27
Hf	5.27	3.85	6.74	5.81	2.85	4.42	1.83	5.41	3.19	3.84	8.77	1.52	3.79
Ta	.75	.59	1.24	1.15	.75	.55	.18	.72	.25	.5	1.16	.46	1.14
Au	45	66	<1	.8	1.4	2180	3.3	3390	.41	5.2	1.1	4630	930
Th	4.27	8.73	9.84	5.80	4.32	3.19	1.96	6.17	5.1	2.27	3.61	1.30	3.14
U	3.47	4.50	9.78	2.71	2.03	4.89	1.42	4.72	4.96	.63	2	2.74	1.66

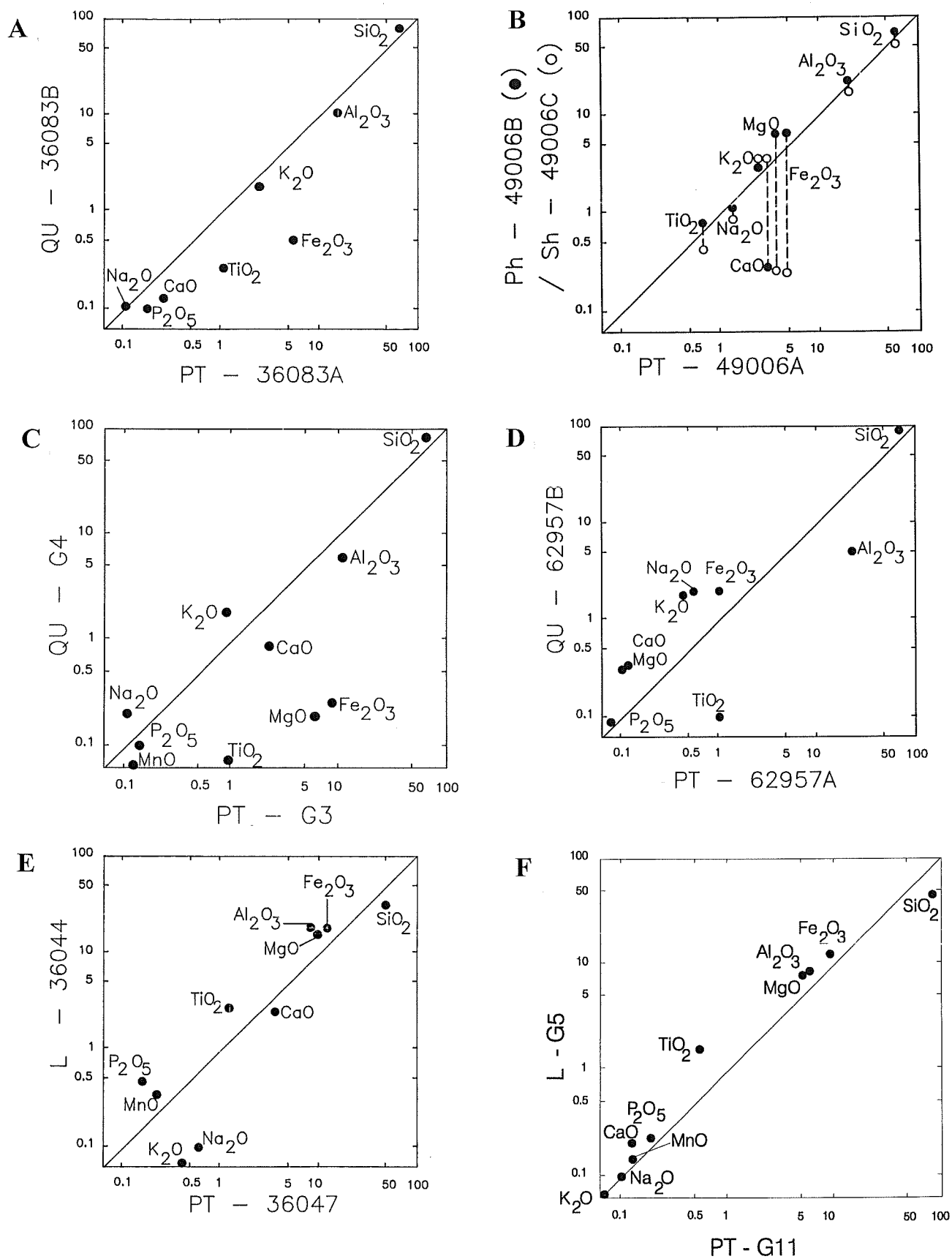


Figure 11: (A-F) Isocon diagrams for major element relationships between host rocks and pseudotachylites from various stratigraphic positions on Western Areas Gold Mine (compare Fig. 2).

Pseudotachylite G3 contains mainly quartz and quartzitic clasts, besides a considerable amount of quartz-carbonate and carbonate inclusions. Carbonate is also abundant as vesicle filling and as matrix segregation. Killick et al. (1988) also determined a CO<sub>2</sub> content of 2 wt% for this sample. Apart from a volatile content which is much higher than that of host rock G4, K and Na are found to be depleted in the breccia (Fig. 11C), and Ca is strongly enriched. Very high Fe, Mg and Al contents in the pseudotachylite, together with the strong depletion in SiO<sub>2</sub>, could be explained with an additional mafic precursor lithology (shale or lava). One would, however, also assume that the whole fault zone was overprinted by a carbonate-rich fluid (depleting SiO<sub>2</sub> and increasing Mg?).

The case of quartzite-hosted pseudotachylite 62957A (Fig. 11D) is principally one of Al enrichment and alkali element addition to the breccia. In the total absence of any petrographic evidence for a contribution from an additional lithic parent, it appears that perhaps the conglomerate could have contributed. Furthermore, some post-pseudotachylite alteration needs to be taken into account, as the sample is cut by a number of < 1 mm quartz or quartz-carbonate veinlets.

Pseudotachylite 36047 is hosted by Ventersdorp lava (Fig. 11E). The breccia is enriched in SiO<sub>2</sub>, and TiO<sub>2</sub> is strongly depleted. As the pseudotachylite was formed directly at the contact between lava and footwall quartzite, mixing between these two lithologies is the logical explanation in this case and is supported by the observed mixed clast population.

The second lava-hosted breccia (G11, Fig. 11F) is also strongly enriched in SiO<sub>2</sub> in comparison with its host rock, and both chemistry and petrography agree well with a mixing model involving lava and quartzite, and perhaps additional minor shale as some clasts were observed. Some Mg and Fe have to be attributed to chlorite present in vesicles and matrix.

The following general conclusions can be drawn: quartzite-hosted pseudotachylites appear depleted in SiO<sub>2</sub>, but enriched in TiO<sub>2</sub>, Al<sub>2</sub>O<sub>3</sub>, and sometimes in Fe<sub>2</sub>O<sub>3</sub> and K<sub>2</sub>O, whereas the lava-hosted breccia is enriched in SiO<sub>2</sub>, with moderate increases in TiO<sub>2</sub>, Fe<sub>2</sub>O<sub>3</sub>, MgO, and Al<sub>2</sub>O<sub>3</sub>, and with variable Ca and alkali element behaviour, for which alteration effects can not be excluded.

### (b) Trace element systematics

Quartzite-hosted pseudotachylite 36083A is strongly enriched in trace elements, particularly in the transition metals Cr, Ni, Zn and Co, but also Sc, Ga, As, Rb, Cs, and Ba. As discussed for the major element data, it is more likely that chemical alteration is seen here rather than the effects of mixing. Similarities in the rare earth element (REE) concentrations of the breccia and host rock support this. The fact that many of the enriched elements are highly mobile or have been found in high concentrations in hydrothermal vein fillings in the Basin (e.g. Zn, Cu, and Ni - Reimold and Boer, 1992, 1993) leads to the conclusion that trace element enrichment in this breccia is probably the result of hydrothermal overprinting.

Most trace elements, including the REEs and many mobile elements, as well as Ni, Au, Th, and U, are strongly enriched in pseudotachylite sample 49006A. Unless an additional precursor rock component (one that is not absolutely demanded by the major element data and that is not evident from the clast record) has been overlooked, these data suggest that either the two identified parent rock types were rather heterogeneous in composition or that post-brecciation alteration again needs to be invoked.

Pseudotachylite G3 is strongly enriched with regard to most trace elements, including strong enrichment of Au, Zn, Ni, Cr, and Pb (Pb after Killick et al., 1988). The petrographic evidence points to alteration by a carbonate-rich fluid. While it appears probable that Au could have been introduced from a reef component in the vicinity of the sample site, the overall chemical make-up of this sample could well be the result of alteration.

For many elements the enrichments observed in sample 62957A are the same as those noted in breccia sample G3, which is also hosted by quartzite. It is unlikely that mixing of very heterogeneous components, such as conglomerates, could result in such similar chemical characteristics.

The two lava-hosted breccia samples 36047 and G11 display different effects from those noted for quartzite-hosted breccias: both samples are depleted with regard to many trace elements, but REEs and many other elements have similar abundances both in the breccia and host rock. This finding does not favour mixing processes as suggested by the major element data, unless components of originally similar trace element compositions were involved. Other elements, including Au, Cr, Co, Ni and Zn, can be either strongly enriched or depleted in the breccia, but also occur in different abundances in the two lava samples. It may be that both breccia and lava were chemically overprinted (compare Henckel and Schweitzer, 1988; Martin, 1988; also: Reimold et al. - VCR studies, in progress).

Figure 12 graphically summarizes the trace element observations. Clearly, breccia enrichment relative to host rock abundances is dominant, though more so for quartzite-hosted breccias than for lava-hosted breccias. Interestingly, those elements (besides Au) that are very enriched, can in other environments be strongly depleted (Cr, Co, Ni, Zn, As, Br). This could be the result of the different availability of these elements in the various sampling areas (for example, base metals may be preferentially available in the vicinity of sulphide-rich reef).

As shown throughout this section, chemical and petrographic evidence for admixture of lithologies other than those analysed is very limited. Consequently, the heterogeneous chemical effects noted here favour the second process, namely alteration/hydrothermal overprinting/element redistribution. In addition to the chemical evidence, macro- and micro-observations (such as veining, alteration halos around fault zones, micropetrographic evidence for pervasive growth of secondary hydrothermal mineralization) for each sample suite support this conclusion.

#### *4. Boskop Dam Drillcore*

The Boskop Dam breccia (Table 4, Figs. 13A-D) compositionally resembles more the lava than the quartzite component. Several elements (Si, Al, K) would favour simple mixing between these end members, but the relatively high concentrations of H<sub>2</sub>O and CO<sub>2</sub> in the breccia zone appear to disturb the actual situation. Carbonate-rich quartzite clasts are abundant in the breccia. Thus, two processes involving carbonate can be envisaged:

- (1) volatiles are derived from a discrete carbonate-rich quartzite layer in contact with the lava, exactly where the breccia was formed; or
- (2) alteration of the lava liberated sufficient carbonate from the altered plagioclase. The

profile shows increasing CO<sub>2</sub> contents in the direction of the lava contact. This trend parallels K<sub>2</sub>O increase and Na<sub>2</sub>O and CaO decrease, further evidence in favour of alteration.

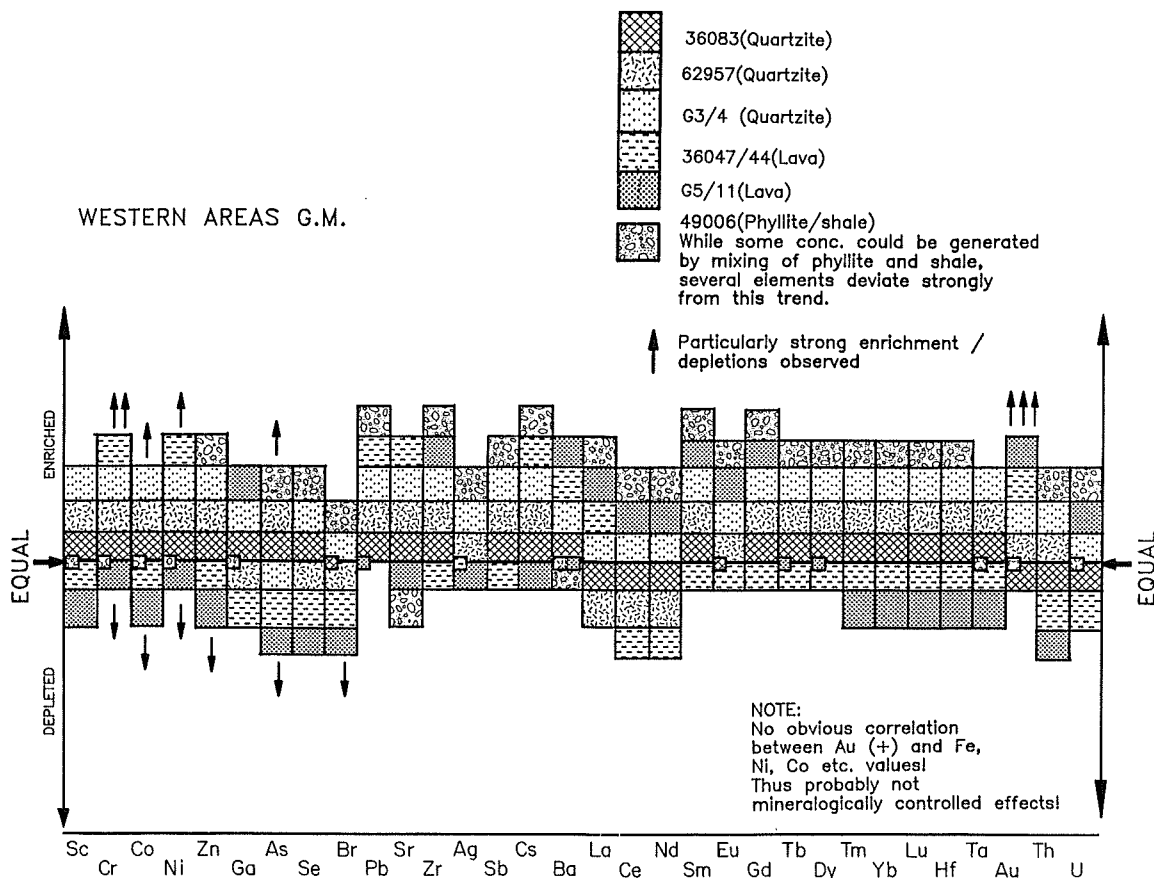


*Figure 12: Relative enrichments or depletions of trace elements in pseudotachylites from Western Areas Gold Mine - in comparison with abundances in the respective host rocks. Where breccia and host rock have similar or equal concentrations, this is indicated by small squares on the abscissa.*

The behavior of most trace elements (Figs. 13B, C) can again be explained by simple two-component mixing. However, Rb, Sr, Cs, Sc, and Sb occur enriched in the breccia and somewhat depleted in the lava. The REEs (Fig. 13C) show a similar trend. From experience with Witwatersrand metasediments and Klipriviersberg lava it can be generalized that metasediment REE patterns are much steeper and elevated to higher abundance levels than observed in the present study (Reimold et al., work in process). Mixing relationships should, thus, be evident in Figure 13 in the form of different slopes for LREE and HREE, as well as by negative correlations across the fault zone. The actual data do not behave in this manner; instead strong REE enrichment is noted for the breccia samples.

The trace elements of Figure 13D display very variable behaviour. For example, Ag is depleted in the fault zone, relative to the country rocks, whereas U, Th, Au, Sc, and Ga are relatively enriched. Cr, Ni, and Zn are heterogeneously distributed in the fault zone and only the Ni and Co data would support a simple mixing model.

**Table 4 :** Compositions of profile samples from borehole BOS7. Data in wt% ( major elements ), ppm ( trace elements ) and ppb ( Au ) ; bd = below detection limit;

\* $\text{Fe}_2\text{O}_3$  = total Fe. Major element data from XRF analysis at Council for Geoscience, Pretoria, Project No. 86/114; trace elements from INAA, analyst C. Koeberl

Sample	7/7	7/6	7/2	7/3	7/4	7/7A
	Quartzite		Pseudotachylite			Lava
$\text{SiO}_2$	89.88	87.70	63.45	64.04	52.65	65.92
$\text{TiO}_2$	bd	bd	.59	.59	1.74	.46
$\text{Al}_2\text{O}_3$	3.17	5.47	12.59	11.91	14.81	13.44
$\text{Fe}_2\text{O}_3$	2.06	1.85	10.53	9.91	10.96	9.94
$\text{MnO}$	bd	.07	.16	.12	.07	bd
$\text{MgO}$	1.16	.72	6.62	6.32	6.08	6.59
$\text{CaO}$	3.10	1.41	3.00	3.69	8.42	.12
$\text{Na}_2\text{O}$	.92	1.95	1.01	1.26	.94	.18
$\text{K}_2\text{O}$	.22	.88	1.52	1.29	3.02	3.09
$\text{P}_2\text{O}_5$	.17	.17	.35	.33	.63	.20
$\text{CO}_2$	2.75	1.42	2.61	2.98	5.07	.30
$\text{H}_2\text{O}^+$	.66	.56	3.77	3.65	3.72	3.80
$\text{H}_2\text{O}^-$	bd	bd	.13	.05	.15	.05
$\text{Sc}$	2.46	2.82	19.5	18.3	34.2	18.0
$\text{Cr}$	118	82	500	480	75.4	880
$\text{Co}$	6.41	7.82	41.8	40.9	75.7	139
$\text{Ni}$	31	55	50	210	76	420
$\text{Zn}$	19.4	17.9	12	124	120	109
$\text{Ga}$	15	9.5	70	170	100	75
$\text{As}$	.85	9	19.9	17.4	12.3	26.2
$\text{Se}$	.09	.4	1	.9	1.6	.3
$\text{Br}$	.3	<.5	.1	<.4	<.9	.2
$\text{Rb}$	16.2	32	63.6	49.2	104	73.1
$\text{Sr}$	70	70	45	120	180	<70
$\text{Zr}$	100	85	170	175	300	160
$\text{Ag}$	.4	.2	.1	.23	<.5	<.4
$\text{Sb}$	.29	.35	1.42	1.2	1.76	.29
$\text{Cs}$	.67	1.21	3.26	2.93	2.88	1.86
$\text{Ba}$	45	160	170	90	240	120
$\text{La}$	14.5	21.6	27.1	27.5	39.6	17.7
$\text{Ce}$	26.3	40.2	59.4	56.7	79.8	37.9
$\text{Nd}$	10	18.4	26.4	26	43.4	17.8
$\text{Sm}$	1.62	2.21	5.17	5.37	9.59	3.8
$\text{Eu}$	.38	.41	1.15	1.07	5.19	.97
$\text{Gd}$	1.8	1.5	7.6	6.5	11.3	3.4
$\text{Tb}$	.33	.27	1.44	1.09	2.04	.62
$\text{Dy}$	1.5	1.45	8.4	6.5	12.1	3.6
$\text{Tm}$	<.1	.1	.51	.49	.9	.32
$\text{Yb}$	.4	.43	2.32	2.41	5.07	1.98
$\text{Lu}$	.068	.068	.365	.351	.733	.287
$\text{Hf}$	2.44	2.27	5.46	5.65	8.14	4.53
$\text{Ta}$	.19	.14	.72	.72	1.06	.87
$\text{Au}$	<2	4.3	4.8	6.2	12	3.9
$\text{Th}$	2.17	2.99	4.81	4.49	3.15	3.63
$\text{U}$	.65	.62	1.91	1.86	1.42	1.01

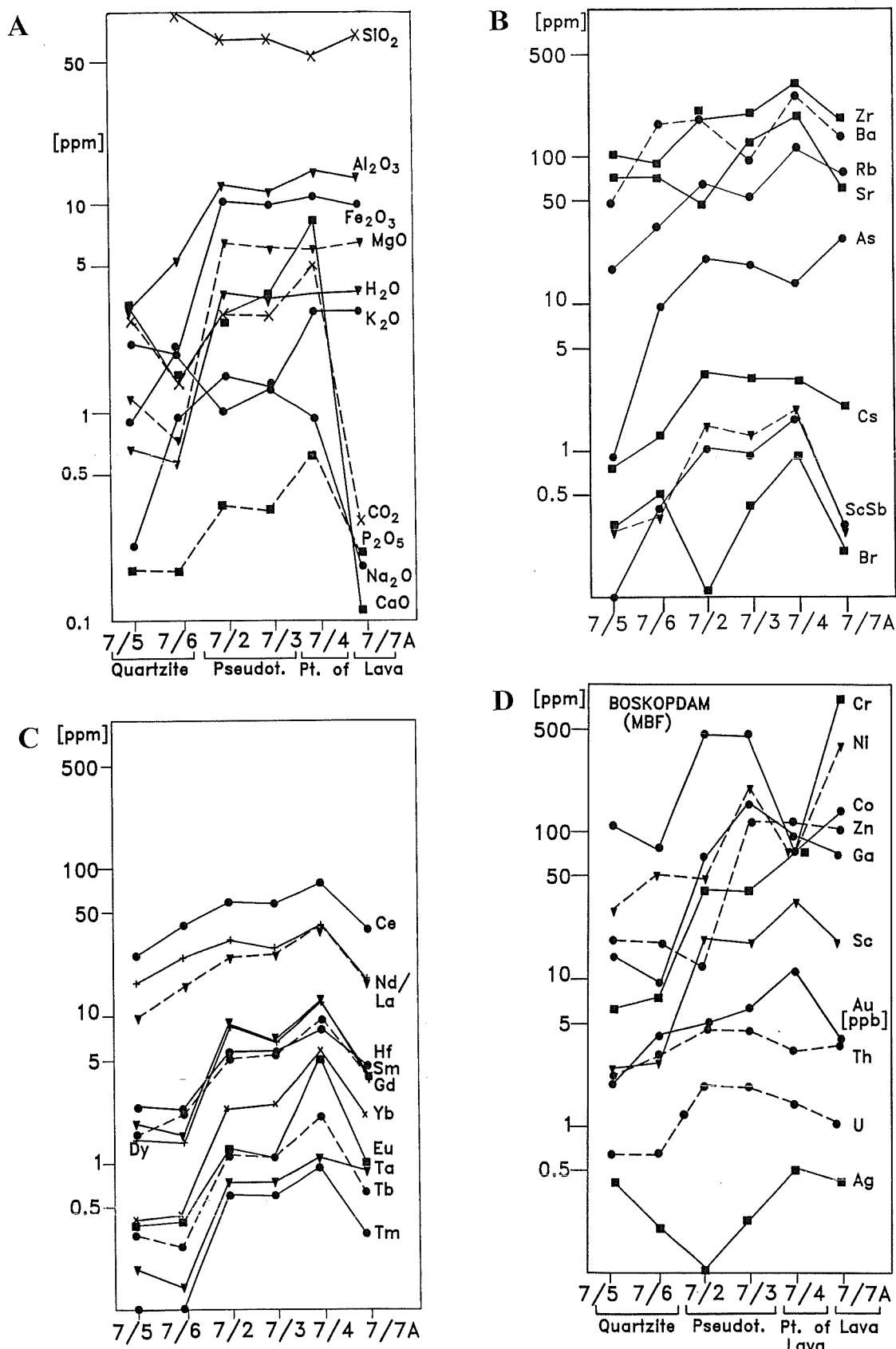


Figure 13: Major (A) and trace element (B-D) profiles across the Master Bedding Fault intersected in borehole BOS7.

## DISCUSSION AND CONCLUSIONS

Several limiting factors need to be considered with regards to this study. Firstly, the underground exposures and drillcore intersections provided only limited access to a knowledge of the overall geological setting of these fault zones. It is possible that not all the lithologies contributing to the development of the breccia were exposed and sampled. Secondly, the complex nature of these fault zones generally allows for the possibility that *more than one deformation and/or alteration event* affected the sections sampled. Evidence for repeated fault movement has been presented earlier and is known from other fault zone intersections in the Witwatersrand Basin. For these reasons, it did not seem appropriate to model volume changes that possibly occurred in these fault zones. A further complicating factor is that several fault rock types usually occur in close association and were either formed simultaneously or at different times.

The high field strength cations, such as Ti, P, Zr, Y, or V, are generally considered to be more immobile than, for example, the alkali elements. However, Killick et al. (1988), Wilshire (1971), and Killick and Reimold (1990) have previously discussed significant enrichment in Pb, as well as enrichments or depletions of other elements in Witwatersrand and Vredefort pseudotachylitic breccias. O'Hara and Blackburn (1989) described a mylonite-bearing deformation zone, in which strong trace element enrichments or depletions were observed. They determined that Ti is indeed a rather immobile element, even under high fluid/rock ratios. Enrichments of P, Zr, Y, and V could be explained by selective mobility of these elements during fluidization. However, the volume loss observed in this mylonitic deformation zone led to removal of SiO<sub>2</sub> and alkali elements.

It is not unlikely that the effects mentioned above are inherent in some of our data. However, the complex interaction between mixing, alteration, and possible volume loss appear difficult to resolve. Nevertheless, this study has shown repeatedly that SiO<sub>2</sub> depletion is not accompanied by alkali element depletion - rather the opposite was observed in some cases.

The sections analysed involve primarily quartz-rich and quartz-poor lithologies. One aspect of importance was to investigate to which degree mixing between different precursor rock types took place at the time of breccia formation. Another process applicable in the formation of tectonic pseudotachylites is the so-called *preferential melting* of specific parent rock minerals during frictional melting (e.g., Reimold, 1991; Spray, 1992). This process has played a role in the formation of pseudotachylites in impact structures (Reimold et al., 1987), including the Vredefort Dome (Reimold, 1991). However, the Vredefort study also proved that the original composition of the precursor rocks is of vital importance with regard to the chemical effects observed when comparing parent rock-breccia pairs. In addition, textural characteristics of the parent rocks, for example grain size and grain shape statistics, or the neighbourhood matrices for parent rock minerals, play a vital role in the determination of the final melt composition.

In summary, the following conclusions can be drawn from this study:

- (1) the East Driefontein profile showed that the Bank Fault-related pseudotachylite was mainly formed by local melting of a specific host rock, but that mixing took place in the interior of the melt zone. Chemical and petrographic evidence indicates limited hydrothermal activity, which demonstrably took place more than once: prior to the formation of pseudotachylite, at the time of its formation, and most likely thereafter. In this context it is noteworthy that breccia sampled

from another intersection of the Bank Fault (in Gold Fields of South Africa borehole E11H, around 2090m depth) consisted of two generations of pseudotachylite, both of which were strongly carbonatised;

- (2) the Doornfontein borehole profile through the Master Bedding Fault is lithologically and chemically complex; both country rocks and breccias are chemically diverse. Typical effects, normally associated with hydrothermal activity, are lacking. It is assumed that mixing of different lithologies, perhaps aided by lateral transport of breccia along this basin-wide fault zone, was the dominant process determining the compositional variation along the profile;
- (3) the pseudotachylite-host-rock pairs from Western Areas Gold Mine displayed different effects in each case. Generally, the breccias are enriched in trace elements. In several cases major and trace element data, combined with petrographic evidence, failed to prove that additional precursor rocks had been neglected. Thus, it is concluded that hydrothermal activity, partially related directly to the breccia-forming event or postdating it, determined the observed chemical systematics. Base metal enrichments were caused by mobilisation and redeposition of material dissolved from country rocks. However, mixing between mafic and felsic precursor rocks was certainly, at least locally, an important process;
- (4) the Boskop Dam profile through the MBF demonstrated that fluid-related processes thoroughly altered the lithologies in this particular fault zone, notably at times of breccia formation. This involved strong alteration of the Ventersdorp lava in the hanging-wall to the fault zone; and
- (5) it has been shown that the chemical properties of several bedding-parallel fault zones have been decisively altered by hydrothermal overprinting. Base metal (including gold) distribution in and along such fault zones was strongly affected, particularly in the fault zones in close contact with reef horizons. Hydrothermal alteration is mainly restricted to the fault zones, but also affected parts of the hanging- and footwall strata.

Several processes were identified as participating in the formation of pseudotachylitic breccia:

- (1) mixing between several precursor rocks was locally important, but it appears that one lithology was apparently dominant;
- (2) preferential melting of specific minerals was important, but this is difficult to quantify in studies of complex fault zones that have been repeatedly affected by secondary processes; and
- (3) autometasomatism of pseudotachylitic matrix, wall-rock alteration, and hydrothermal alteration at post-pseudotachylite formation times all played a significant role. The latter process was responsible for extensive sulphide mineralisation in joints and shear zones, whereas autometasomatism can be recognised by sulfide and other deposits in the matrices of breccias.

Future work must involve the determination of the nature of the fluids involved in these processes. Boer et al. (1993a, b; cf. also Reimold and Boer, 1991, 1992) determined that several fluids were active around the time of breccia formation in different parts of the Witwatersrand Basin (as along the West Wits Line and in the West Rand goldfield). This suggests that fluids were locally

generated and active. However, much more work is needed to refine the knowledge of fluids, their activities, and the times at which they were active.

The current geochronological data base strongly favours major fluid activity at times just before 2 Ga ago. In detail, these data favour a strong Vredefort impact-related effect on major parts of the Basin. However, activity related to the emplacement of the Bushveld Complex can not be excluded. Other results, such as the findings of rare authigenic zircons (Frimmel, 1997) and U-Pb isotopic analysis of Witwatersrand kerogen (Robb et al., 1994) indicate hydrothermal overprinting at ca. 2.3 Ga ago, perhaps involving fluids derived from the Transvaal sedimentary basin. Others promote a major hydrothermal, ore-forming event during Ventersdorp times (ca. 2.7 Ga ago; e.g., Barnicoat et al., 1997). It is difficult to obtain unambiguous chronological information in the complex, multideformed and overprinted situation as is presented in the Archaean Witwatersrand Basin. This is especially so if significant thermal/hydrothermal events occurred relatively late in the evolution of the Basin, such as with the Kibaran/Namaquan and Vredefort events at 1-1.2 Ga and 2.02 Ga, respectively (Reimold and Gibson, 1996 for a review of relevant literature; also Robb et al., 1998). Further petrographic and chronological studies have the potential to refine the multi-stage evolution of the Witwatersrand Basin, the timing of ore-forming events, and the processes involved therein.

—oOo—

### ACKNOWLEDGEMENTS

The authors are indebted to the following companies and individuals: Gold Fields of South Africa Limited and Johannesburg Consolidated Investment Company Limited, for making chemical data available and for permission to publish these results; these companies and the mine managements and geological staff of Doornfontein, and Western Areas Gold Mines, for permission to sample underground as well as drillcore, and for logistical support; the Director of the Council for Geoscience for analytical sponsorship of project 86/114; Lyn Whitfield, Di Du Toit, and Mark Hudson of the Department of Geology, University of the Witwatersrand, for technical support. WUR's research is funded by an Open Research Programme grant by the Foundation for Research Development.

### REFERENCES

- Barnicoat, A.C., Henderson, I.H.C., Knipe, R.J., Yardley, B.W.D., Napier, R.W., Fox, N.P.C., Kenyon, A.K., Muntingh, D.J., Strydom, D., Winkler, K.S., Lawrence, S.R., and Cornford, C., 1997. Hydrothermal gold mineralization in the Witwatersrand basin. *Nature*, **386**, 820-824.
- Berlenbach, J.W. and Roering, C., 1992. Sheath-fold-like structures in pseudotachylites. *J. Struct. Geol.*, **14**, 847-846.
- Boer, R.H., Reimold, W.U., and Graney, J.R., 1993a. Fluid inclusion gas analyses of the Ventersdorp Contact Reef, Witwatersrand Basin, South Africa. Conf. on *Min. Explor. '93*, Cape Town, August 1993, 2pp.
- Boer, R.H., Reimold, W.U., and Graney, J.R., 1993b. Physico-chemical conditions of gold remobilization in the Ventersdorp Contact Reef, Witwatersrand Basin. Symp. *The VCR Revisited*, August 1993, Carletonville, West. Tvl. Branch, Geol. Soc. S. Afr., pp.92-94.
- Davidson, G., 1995. After the gold rush. *New Scientist*, **1973**, 26-31.
- Dressler, B.O., 1984. The effects of the Sudbury Event and the intrusion of the Sudbury Igneous Complex on the footwall rocks of the Sudbury Structure. In *The Geology and Ore deposits of the Sudbury Structure* (eds. E.G. Pye, A.J. Naldrett, and P.E. Giblin), Ontario Geol. Survey Spec. Pap., **1**, pp.97-136.
- Fletcher, P. and Reimold, W.U., 1989. Some notes and speculations on the pseudotachylites in the Witwatersrand Basin and the Vredefort Dome. *S. Afr. J. Geol.*, **92**, 223-234.
- Frimmel, H.E., 1997. Detrital origin of hydrothermal Witwatersrand gold - a review. *Terra Nova*, **9**, 192-197.
- Gibson, R.L., Armstrong, R.A. and Reimold, W.U., 1997. The age and thermal evolution of the Vredefort impact structure: A single-grain U-Pb zircon study. *Geochim. Cosmochim. Acta*, **61**, 1531-1540.
- Grieve, R.A.F., Coderre, J.M., Robertson, P.B. and Alexopoulos, J., 1990. Microscopic planar

deformation features in quartz of the Vredefort structure: Anomalous but still suggestive of an impact origin. *Tectonophys.*, **171**, 185-200.

Grieve, R.A.F., Stöffler, D. and Deutsch, A., 1991. The Sudbury Structure: controversial or misunderstood? *J. Geophys. Res.*, **96**, 22753-22764.

Hart, R.J., Andreoli, M.A.G., Reimold, W.U. and Tredoux, M., 1991. Aspects of the dynamic and thermal metamorphic history of the Vredefort cryptoexplosion structure: implications for its origin. *Tectonophys.*, **192**, 313-331.

Henckel, J. and Schweitzer, J.K., 1988. Geochemical and mineralogical characteristics of two different depositional events within a portion of the Ventersdorp Contact Reef at Elandsrand Gold Mine, and their implications on provenance controlled facies delineation (Ext. Abstr.). *Ventersdorp Contact Reef Symposium*, Western Tvl. Branch, Geol. Soc. S. Africa, Potchefstroom, pp.51-54.

Henkel, H. and Reimold, W.U., 1997. Integrated gravity and magnetic modelling of the Vredefort impact structure - Reinterpretation of the Witwatersrand Basin as the erosional remnant of an impact basin. *Econ. Geol. Res. Unit. Inf. Circ.*, **296**, Univ. of the Witwatersrand, 89pp.

Henkel, H. and Reimold, W.U., 1998. Integrated geophysical modelling of a giant, complex impact structure: anatomy of the Vredefort Structure. *Tectonophys.*, **287**, 1-20.

Kamo, S.L., Reimold, W.U., Krogh, T.E., and Colliston, W.P., 1996. A 2.023 Ga age for the Vredefort impact event and a first report of shock metamorphosed zircons in pseudotachylitic breccias and Granophyre. *Earth Planet. Sci. Lett.*, **144**, 369-388.

Killick, A.M. and Reimold, W.U., 1990. Review of the pseudotachylites in and around the Vredefort Dome, South Africa. *S. Afr. J. Geol.*, **93**, 350-365.

Killick, A.M. and Roering, C., 1998. An estimate of the physical conditions of pseudotachylite formation in the West Rand Goldfield, Witwatersrand Basin, South Africa. *Tectonophys.*, **284**, 247-259.

Killick, A.M., Thwaites, A.M., Germs, G.J.B. and Schoch, A.E., 1988. Pseudotachylite associated with a bedding-parallel fault zone between the Witwatersrand and Ventersdorp Supergroups, South Africa. *Geol. Rdsch.*, **77**, 329-344.

Koeberl, C., Kluger, F. and Kiesl, W., 1987. Rare earth element determinations at ultra-trace abundance levels in geologic materials. *J. Radioanal. Nucl. Chem.*, **112**, 482-487.

Leroux, H., Reimold, W.U., and Doukhan, J.-C., 1994. A T.E.M. investigation of shock metamorphism in quartz from the Vredefort dome, South Africa. *Tectonophys.*, **230**, 223-239.

Maglaughlin, J.F. and Spray, J.G., (eds.), 1992a. Frictional Melting Processes and Products in Geological Materials. *Tectonophys.*, **204**, 337pp.

Maglaughlin, J.F. and Spray, J.G., 1992b. Frictional melting processes and products in geological

materials: introduction and discussion. *Tectonophys.*, **204**, 197-206.

Martin, G.J., 1988. Some mineralogical observations of the Ventersdorp Contact Reef at the Leeudoorn Division of Kloof Gold Mining Company (Ext. Abstr.). *Ventersdorp Contact Reef Symposium*, Western Tvl. Branch, Geol. Soc. S. Africa, Potchefstroom, pp.55-59.

Minter, W.E.L., Goedhart, M., Knight, J. and Frimmel, H.E., 1993. Morphology of Witwatersrand gold grains from the Basal Reef: evidence for their detrital origin. *Econ. Geol.*, **88**, 237-248.

O'Hara, K. and Blackburn, W.H., 1989. Volume-loss model for trace element enrichments in mylonites. *Geology*, **17**, 524-527.

Phillips, G.N. and Myers, R.E., 1989. The Witwatersrand Gold Fields: Part II. An origin for Witwatersrand gold during metamorphism and associated alteration. *Econ. Geol. Mon.*, **6**, pp.598-608.

Reimold, W.U., 1990. The controversial microdeformations in quartz from the Vredefort structure, South Africa. *S. Afr. J. Geol.*, **93**, 645-663.

Reimold, W.U., 1991. Geochemistry of pseudotachylites from the Vredefort Structure, South Africa. *N. Jahrb. Mineral. Abh.*, **161**, 151-184.

Reimold, W.U., 1995. Pseudotachylite - generation by friction melting and shock brecciation? - A review and discussion. *Earth-Science Rev.*, **39**, 247-264.

Reimold, W.U., 1998. Exogenic and endogenic breccias: a discussion of major problematics. *Earth-Science Rev.*, **43**, 25-47.

Reimold, W.U. and Boer, R.H., 1992. Final Report to Anglo American Prospecting Services on results in the *Ventersdorp Contact Reef Pseudotachylite Geochemical Project* (1991-1992), Dept. of Geol., Univ. of the Witwatersrand, Johannesburg, 186pp.

Reimold, W.U. and Boer, R.H., 1993. Final Report to Anglo American Prospecting Services on Results in the *Ventersdorp Contact Reef Pseudotachylite Geochemical Project* (Extension 1992-1993), Dept. of Geol., Univ. of the Witwatersrand, Johannesburg, 133pp.

Reimold, W.U. and Colliston, W.P., 1994. Pseudotachylites of the Vredefort Dome and the surrounding Witwatersrand Basin, South Africa. In: *Large Meteorite Impacts and Planetary Evolution (Sudbury 1992)*, B.O. Dressler, R.A. F. Grieve, and V.L. Sharpton (eds.), *Geol. Soc. Amer. Spec. Pap.*, **293**, pp.177-196.

Reimold, W.U. and Gibson, R.L., 1996. Geology and evolution of the Vredefort impact structure, South Africa. *J. Afr. Earth Sci.*, **23**, 125-162.

Reimold, W.U. and Koeberl, C., 1991. Chemical relationships between Witwatersrand pseudotachylites and their host rocks: evidence for fault-controlled hydrothermal activity? *VI. Meet. Europ. U. Geosciences*, Strasbourg, *Terra Abstr.*, **3**, p.386.

Reimold, W.U., Oskierski, W. and Huth, J., 1987. The pseudotachylite from Champagnac in the Rochechouart meteorite crater, France. *Proc. Lunar Planet. Sci. XVII, J. Geophys. Res.*, **92**, B4, 737-748.

Robb, L.J. and Meyer, F.M., 1991. A contribution to recent debate concerning epigenetic versus syngenetic mineralization processes in the Witwatersrand Basin. *Econ. Geol.*, **86**, 396-401.

Robb, L.J. and Meyer, F.M., 1995. The Witwatersrand Basin, South Africa: Geological framework and mineralization processes. *Ore Geol. Rev.*, **10**, 67-94.

Robb, L.J., Landais, P., Meyer, F.M., and Davis, D.W., 1994. Nodular organic matter in granites: implications for the origin of 'kerogen' in the Witwatersrand Basin, South Africa. *Explor. Min. Geol.*, **3**, 219-230.

Robb, L.J., Charlesworth, E.G., Drennan, G.R., Gibson, R.L. and Tongu, E.L., 1997. Tectono-metamorphic setting and paragenetic sequence of Au-U mineralisation in the Archaean Witwatersrand Basin, South Africa. *Austral. J. Earth Sci.*, **44**, 353-371.

Robb, L.J., Armstrong, R.A. and Waters, D.J., 1998. Nature and duration of mid-crustal granulite facies metamorphism and crustal growth: Evidence from single zircon U-Pb geochronology in Namaqualand, South Africa. *Econ. Geol. Res. Unit. Inf. Circ.*, **323**, Univ. of the Witwatersrand, Johannesburg, 38pp.

Shand, S.J., 1916. The pseudotachylyte of Parijs (Orange Free State), and its relation to "trap-shotten gneiss" and "flinty crush-rock". *Geol. Soc. London Quart. J.*, **72**, 198-221.

Spray, J.G., 1992. A physical basis for the frictional melting of some rock-forming minerals. *Tectonophys.*, **204**, 205-221.

Spray, J.G., Kelley, S.P. and Reimold, W.U., 1995. Laser-probe  $^{40}\text{Ar}$ - $^{39}\text{Ar}$  dating of pseudotachylites and the age of the Vredefort impact event. *Meteoritics*, **30**, 335-343.

Trieloff, M., Reimold, W.U., Kunz, J., Boer, R.H. and Jessberger, E.K., 1994.  $^{40}\text{Ar}$ - $^{39}\text{Ar}$  thermochronology of pseudotachylites at the Ventersdorp Contact Reef, Witwatersrand basin. *S. Afr. J. Geol.*, **97**, 365-384.

Wilshire, H.G., 1971. Pseudotachylite from the Vredefort Ring, South Africa. *J. Geol.*, **79**, 195-206.